MASTERARBEIT | MASTER'S THESIS

Titel | Title

Evaluating Prebiotic Activity of Arabinogalactan on the Human Gut Microbiome

verfasst von | submitted by

Sanaz Khadem

angestrebter akademischer Grad | in partial fulfilment of the requirements for the degree of

Master of Science (MSc)

Wien | Vienna, 2024

Studienkennzahl lt. Studienblatt | Degree programme code as it appears on the student record sheet:	UA 066 830
Studienrichtung lt. Studienblatt | Degree programme as it appears on the student record sheet:	Masterstudium Molecular Microbiology, Microbial Ecology and Immunobiology
Betreut von | Supervisor:	Univ.-Prof. David Berry Privatdoz. PhD

Acknowledgements

I would like to express my sincere gratitude to Prof. David Berry for allowing me to be part of his incredible group and for his constant support throughout this project and our various collaborations. His mentorship has been invaluable, and I have learned so much from him, helping me to gain confidence in myself and recognize my potential.

I am deeply thankful to Hamid Rasoulimehrabani, MSc, for his generous guidance and supervision during my master's thesis. His teachings and encouragement have been instrumental in driving my success.

I would also like to extend my thanks to Miriam Philipp for conducting and analyzing the Raman microspectroscopy experiments. Special thanks to Rebecca Gallo for her assistance with anaerobic incubation, Georgi Nikolov for his laboratory support, Dr. Marc Mußmann for his help with the FACS settings, and Dr. Márton Palatinszky for his assistance with the RACS experiments.

Lastly, I am grateful to all the members of the Gut Group for their constant support, friendliness, and for making the group feel like home. Their encouragement has been a significant part of this journey.

Abstract

Arabinogalactan (AG), a polysaccharide with prebiotic potential, was evaluated for its impact on the gut microbiota. The fecal samples from 10 healthy human donors were analyzed using advanced culture-independent techniques. These included Bioorthogonal Noncanonical Amino Acid Tagging (BONCAT) and Fluorescence Activated Cell Sorting (FACS), using L-azidohomoalanine (AHA) as a marker for cell activity. Additionally, Raman microspectroscopy and Raman Activated Cell Sorting (RACS) with heavy water (D_2O) were employed to track metabolically active bacteria. AG significantly influenced both the overall microbial community and the active fraction in anaerobic *in vitro* incubations, promoting the growth of commensal and beneficial taxa such as *Bifidobacterium*, *Bacteroidetes*, *Faecalibacterium*, *Parabacteroides*, *Phascolarctobacterium*, and *Blautia*. Despite inter-individual variability in metabolic activity, consistent results were observed across several genera. RACS analysis further led to the isolation of a wide range of AG-degrading strains, in line with earlier results, primarily from the genera *Bifidobacterium* and *Collinsella*, as well as from genera such as *Alistipes*, *Bacteroides*, *Catenibacterium*, *Dysosmobacter, Eggerthella*, *Faecalibacterium*, *Parabacteroides*, *Phascolarctobacterium*, *Phocaeicola*, and *Ruminococcus*. Additionally, AG was shown to foster the growth of microbes associated with gut health, immune modulation, and potentially cognitive function, presenting opportunities for future targeted therapeutic applications. These findings demonstrated AG's role in enhancing beneficial microbial populations and support its potential use in developing next-generation probiotics or prebiotic supplements. Further studies exploring enzyme activity and microbial interactions are recommended to fully understand AG's broader health implications.

Table of Contents

Chapter 1: Introduction

1.1 Gut microbial Composition and its Role in the human body

The human gut hosts approximately 10^{13} microbial cells, outnumbering human cells, and shapes a complex ecosystem of microbial populations [1]. Taking into account the diverse microorganisms, including bacteria and archaea, as well as, fungi, viruses, and protozoa, led to the introduction of the concept of 'microbiota' in the early 20th century [2], [3]. In contrast, “Microbiome” is a term that refers to microbial communities, collective genetic material, their physical and chemical environment, and the metabolites they produce, providing a broader concept than microbiota [2].

Shaping of the gut microbiota is first affected by factors at the early life including birth approach (vaginal birth or cesarean), initial feeding practices (breastfeeding or formula feeding), and antibiotic consumption [4], [5]. These early influences help establish the foundational microbial community in the gut. In adulthood, diet, antibiotics and medications, lifestyle, environmental factors, age, hormonal changes, geographical region, and health conditions can further shape and alter the gut microbiota composition [6], [7], [8]. Among the eukaryotic and prokaryotic cells that inhabit the large intestine, bacteria are the most abundant microorganisms, predominantly belonging to the *Firmicutes* and *Bacteroidetes* phyla, along with two other *Proteobacteria* and *Actinobacteria* phyla. [9], [10]. It is worth mentioning that the taxonomic classification names have recently changed. For example, Firmicutes has been renamed to Bacillota, and Proteobacteria has been renamed to Pseudomonadota [11]. However, in this study, the former names were used to avoid confusion and maintain consistency with the majority of existing literature.

The microbial residents of the gut are not isolated communities; rather, they engage in bi-directional relationships with other organs and systems in the body. These interactions create an orchestral harmony that is crucial for the host's homeostasis and overall health [12]. This complex network of communications influences processes such as metabolism,

immune function, and mental health, highlighting the gut microbiome's essential role in different functions [13].

The main roles of the gut microbiome are participating in the digestion of food and nutrient absorption. The microbial enzymes have the ability to degrade complex proteins, lipids, and carbohydrates and facilitate the extraction of nutrients that the human body cannot metabolize independently. [14]. For example, the small intestine cannot digest dietary fibers, however, colonic microflora degrades them by fermentation and produces short-chain fatty acids (SCFAs) including butyrate, acetate, and propionate as by-products [15]. SCFAs provide energy to colon cells, promote gut health, reduce inflammation, and play an important role in regulating metabolic homeostasis [16], [17]. Additionally, these microorganisms are important players in the production of vitamins B and K, hormones such as serotonin and lysine, tryptophan, and threonine amino acids [18], [19] .

Beyond its role in nutrient metabolism, the gut microbiome interacts with various other systems and organs, notably the immune system. It helps in the development and maturation of immune cells, producing antimicrobial compounds and acts as a barrier against pathogenic organisms [20], [21]. This protective role is crucial for preserving the gut barrier's integrity and preventing colonization of pathogens and proper response to harmful substances, which could otherwise trigger systemic infections and inflammation [22].

These interactions are also connected to the gut-brain axis, a bidirectional pathway between the gut and brain that is linked by the vagus nerve [23]. It involves neurological, hormonal, and immunological signaling pathways and crucial role of microbiota. These microorganisms by synthesizing neurotransmitters such as serotonin and gamma-aminobutyric acid (GABA), which have profound effects on mental health and cognitive processes.[24], [25]. On the other side of the connection, psychiatric disorders, mood changes, and stress prompt the brain to produce signals that can disrupt gut integrity, interfere with digestion, and alter the composition of its microbial populations [23].

1.2 Dysbiosis

Maintaining stable microbial communities is crucial for ensuring their proper function and their role in human health. Various factors, such as dietary intake changes, infections, antibiotic use and stress, can change the composition of natural gut microbiota, leading to a condition known as dysbiosis [26]. Dysbiosis typically results in a decrease in overall gut microbiota diversity, which is a critical marker of a healthy microbiome. A diverse microbial population is more resilient and better prepared to maintain homeostasis in stressful conditions. Conversely, reduced diversity makes the gut more susceptible to colonization by pathogenic bacteria and diminishes its ability to carry out essential functions, potentially triggering a cascade of health problems [8].

For instance, the ratio of *Bacteroidetes* to *Firmicutes* is an important biomarker for assessing gut health. Studies have demonstrated that in the development of gallstone disease (GSD), this ratio shifts toward an increased abundance of *Firmicutes* and a depletion of Bacteroidetes [27]. A similar pattern has been shown in inflammatory bowel disease (IBD) patients, characterized by a decrease in gut microbiota diversity due to an increase in *Firmicutes* and *Actinobacteria* [28]. In addition, these patients typically show a reduced abundance of beneficial bacteria such as *Faecalibacterium prausnitzii* and *Bifidobacterium* species. *F. prausnitzii* is particularly important due to its anti-inflammatory effects, while *Bifidobacterium* species are known for their role in promoting gut health through the production of SCFAs and inhibition of pathogenic bacteria [29]. The depletion of these beneficial microbes, makes an ecological niche left open that can be occupied by opportunistic pathogens such as *Escherichia coli*, and *Bilophila* [29], [30]. These pathogenic bacteria can proliferate under such conditions, leading to an increase in their numbers and production of pro-inflammatory molecules and toxins, which can aggravate the intestinal environment and contribute to the chronic nature of IBD.

The gut microbiota plays significant role in brain health and its fingerprint can be found in mental disorders due to imbalance composition. Alterations in specific bacteria are associated with different brain related and psychiatric disorders. These changes can

influence inflammation, gut barrier function, and neurotransmitter production, all of which are important in the pathogenesis and development of brain-related diseases including anxiety, Parkinson's disease, depression, Alzheimer's, and autism [25], [31]. For example, individuals living with Alzheimer's disease are positively associated with higher levels of pro-inflammatory bacteria like *Escherichia/Shigella* and *Proteobacteria*. In contrast, bacteria like *Eubacterium rectale*, *F. prausnitzii*, and *Bifidobacterium*, which are involved in anti-inflammatory actions, are found to be depleted.[32]. People who suffer from mental conditions such as anxiety, depression, and stress often exhibit a reduced abundance of beneficial bacteria like *Faecalibacterium* and *Bacteroidetes* (important players in SCFAs production), while showing enrichment in possibly pathogen bacteria like *Prevotella* and *Streptococcus* (participate in inflammatory cytokines metabolization). These microbial shifts contribute to the inflammatory processes and gut-brain axis disruptions associated with these conditions.[33].

Considering the critical role of a balanced gut microbiome in human health, finding solution for dysbiosis is essential for preventing and managing a range of health conditions. Nonetheless, it is essential to recognize that the interplay between these microbes and various parts of the body are bi-directional and they are constantly influenced by each other. Therefore, understanding this complexity should be considered for developing effective treatments that target not only the gut but also the broader physiological networks that maintain health. One promising strategy for restoring microbial balance is the use of probiotics and prebiotics.

1.3 Probiotics and Prebiotics

To support and enhance the beneficial roles of the gut microbiome, the concepts of probiotics and prebiotics have drawn a lot of interest in recent years. Probiotics are defined as "live microorganisms which, when administered in adequate amounts, confer a health benefit on the host" by the World Health Organization and the Food and Agriculture

Organization of the United Nations [34]. This definition emphasizes the importance of these beneficial microbes in promoting health through the modulation of the host's microbiota. Common probiotic strains consist of *Lactobacillus* species (e.g., *L. rhamnosus*, *L. acidophilus*), *Bifidobacterium* species (e.g., *B. longum*, *B. infantis*), *Saccharomyces boulardii*, and *Streptococcus thermophilus* [35]. Probiotics can help restore balance to the gut ecosystem, especially following disruptions caused by different factors that earlier were mentioned.

L. rhamnosus GG (LGG) and *B. infantis* are two well-researched probiotics that offer significant benefits for both gastrointestinal disorders like IBD and mental health issues such as anxiety. LGG is renowned for its ability to enhance gut barrier function, modulate gut microbiota, and exert anti-inflammatory effects, which are crucial in managing IBD. Additionally, it interacts with the gut-brain axis by producing neurotransmitter-like substances and modulating stress hormones, thereby helping to reduce anxiety and stress. *B. infantis*, on the other hand, is particularly effective in reducing systemic inflammation, a key factor in both IBD and anxiety. It modulates the immune response, lowers inflammatory markers, and also influences the gut-brain axis, which may explain its positive effects in mental health [36], [37].

Another example is *S. boulardii*, that, by competing with pathogens and enhancing gut health, can also help IBD patients and people who suffer from diarrhea [38]. In brain and cognitive disorders like Alzheimer's Disease, it has been found that a cocktail of *L. fermentum, L. casei* and *L. acidophilus* probiotics reduced amyloid plaques and improve cognitive function [39].

However, for probiotics to exert their beneficial effects effectively, they require specific nutrients to thrive and proliferate. This is where prebiotics come into play. Although the definition of prebiotics has evolved, it was first articulated in 1995 by Gibson and Roberfroid as "a non-digestible food ingredient that beneficially affects the host by selectively stimulating the growth and/or activity of one or a limited number of bacteria in the colon"

[40]. Prebiotics act as a vital food source for probiotics, fostering a healthy and balanced microbiome by encouraging the growth of beneficial bacterial populations.

Research has consistently demonstrated that dietary intake of prebiotics can lead to positive changes in gut microbiota composition. This selective stimulation often favors the growth of beneficial bacteria, especially from the *Bifidobacterium* and *Lactobacillus* genera [41], [42]. These genera are crucial for maintaining gut health, as they contribute to the SCFAs production that play vital roles in controlling inflammation and promoting immune function [43]. Moreover, prebiotics can enhance the resilience of probiotics by protecting them from oxidative stress and the harsh environment of bile acids during gastrointestinal transit. This protection not only ensures the viability of probiotics but also significantly enhances their overall effectiveness in maintaining a healthy gut microbiome [41]. By synergistically working together, probiotics and prebiotics contribute to a robust and dynamic microbial ecosystem, ultimately supporting the host's health and well-being. This interplay highlights the importance of a balanced diet rich in both probiotics and prebiotics to foster optimal gut health.

1.3.1 Examples of prebiotics

Various types of prebiotics have been identified and extensively studied, including xylooligosaccharides (XOS), inulin, fructooligosaccharides (FOS), galactooligosaccharides (GOS), and lactulose [42], [44], [45], [46], [47]. Each of these prebiotics differs in its chemical structure, source, and effectiveness in modulating the gut microbiome population. For instance, XOS are products from hydrolysis of xylan, a component of plant cell walls, and have been shown to enhance the growth of probiotics such as *Bifidobacterium* and *Lactobacillus* [44]. Inulin, a naturally occurring polysaccharide found in many plants, particularly in chicory root, is another well-studied prebiotic. It is known for its ability to promote the growth of *Bifidobacteria*, that are key players for maintaining gut health [42]. FOS, similar to inulin, are composed of fructose units and are found in various fruits and vegetables [45]. They are particularly effective at stimulating the growth of beneficial bacteria and relate to a balanced gut microbiome. GOS are derived from lactose and are

prevalent in human milk, highlighting their importance in the development of a healthy gut microbiome in infants. This prebiotic has been demonstrated to enhance the growth of *Bifidobacteria* and other beneficial bacteria, thereby supporting immune function and overall gut health [46].

Lactulose, a synthetic disaccharide, is another prebiotic that has garnered attention for its effects on abundances of beneficial bacteria while simultaneously preventing the growth of pathogens. It is frequently used in clinical practice to treat condition like hepatic encephalopathy and chronic constipation due to its beneficial effects on the gut microbiota [47].

The effectiveness of these prebiotics in modulating the gut microbiome depends on various factors, including their chemical structure, the specific strains inhabit in the colon, and the overall diet of the individual. For example, while inulin and FOS are both fructans, their degree of polymerization can affect how they are fermented by gut bacteria, leading to different outcomes in terms of microbial growth and metabolic activity [48].

These diverse prebiotics underscore the importance of a diverse diet, high in many forms of fibers and non-digestible carbohydrates to support a healthy and balanced gut microbiome. By supplementing the diet with different prebiotics, individuals can foster a more resilient and diverse microbial community, which is vital for supporting overall health and preventing disease.

1.4 Arabinogalactan as the candidate prebiotic of this study

One such prebiotic is arabinogalactan (AG), a polysaccharide primarily presents in the cell walls of larch trees and various vegetables. This complex indigestible compound comprises a backbone of galactose units with arabinose side chains [49]. Arabinogalactan is a type of hemicellulose, a class of complex carbohydrates that cannot be absorbed in the human gastrointestinal tract or hydrolyzed by host enzymes and has been studied for its prebiotic potential. As such, it reaches the colon intact and the gut microbiota ferment it [50].

Arabinogalactan has been shown to produce lactic acid, succinic acid, and SCFAs including acetate, propionate and butyrate during fermentation in colon [51] by stimulating the growth of commensal bacteria in the gut. For instance, it has the potential to serve as a nutrient source for probiotics, particularly *Bifidobacterium* and *Bacteroidetes*, alter gut microbiome composition, and modulate immune responses arabinogalactan [51], [52], [53]. This prebiotic activity supports the maintenance of a balanced gut microbiome, that is critical for general health and digestive system. Arabinogalactan contributes to gut barrier integrity by enhancing the growth of such bacteria, followed by production of SCFA, which, in turn, support the maintenance of epithelial cells tight junctions in the gut lining [51].

Beyond its impact on gut microbiota, AG also exhibits immunomodulatory properties. Studies suggest that arabinogalactan can enhance immune response by stimulating the performances of macrophages, natural killer (NK) cells, and components that are important players of the innate immune system. The findings indicated that arabinogalactan supplementation led to increased NK cell activity and enhanced the body's ability to cope with infections [53], [54]. Additionally, arabinogalactan has been linked to the modulation of cytokine production and the immune response is significantly influenced by these signaling molecules. By influencing cytokine production, AG can help balance pro-inflammatory and anti-inflammatory responses, potentially eliminating the possibility of chronic inflammatory conditions [55].

Studying compounds with prebiotic activity is crucial for developing targeted dietary strategies and efficient foods that can improve human health. This study focused on evaluating the prebiotic activity of AG by using culture-independent methods.

1.5 The Study Techniques

In recent years, applying culture-independent methods instead of cultivating the microbes in laboratory, has significantly increased. Traditional methods are based on isolating and

growing microorganisms in controlled laboratory conditions. Although these methods have been instrumental in identifying and characterizing many microorganisms, they have notable drawbacks. One of the limitations is their inability to capture the full diversity of the gut microbiota. Many microorganisms in the gut are challenging to culture due to their growth requirements or dependencies on other microbes. This often results in an incomplete representation of microbial diversity, where only the most easily cultured species are detected. Additionally, culture-based methods can introduce biases in microbial representation. Fast-growing and easily cultivable species are more likely to be overrepresented, while less abundant or more complex species may be underrepresented or entirely missed. Furthermore, culturing microorganisms outside their natural environment can alter their physiological state and interactions, leading to a loss of context regarding their ecological roles and interactions within the gut microbiome [56], [57]. These limitations underscore the need for alternative approaches that can provide a more comprehensive and accurate insight of the gut microbiota populations. Non-cultivation-based techniques such as metagenomics, stable isotope probing (SIP), and Fluorescence In Situ Hybridization (FISH) have emerged as powerful tools to overcome these challenges, offering deeper insights into microbial diversity, functionality, and dynamics [58], [59].

This study used different culture-independent and culture-dependent methods to identify arabinogalactan utilizer from the human gut bacterium.

1.5.1 BONCAT-FACS

Bioorthogonal Noncanonical Amino Acid Tagging (BONCAT) is a method that utilizes L-azidohomoalanine (AHA) for tagging proteins [60]. AHA, a noncanonical amino acid analogous to methionine and is not naturally present in cellular protein synthesis. However, when added to growth media, AHA is incorporated into proteins of metabolically active cells, enabling selective labeling for click chemistry. AHA contains an azide group ($-N_3$) that participates in bioorthogonal chemical reactions with chemical groups attached to alkyne-

modified dyes. The click chemistry reaction is facilitated by Cu(I) ions, which act as a catalyst for the azide-alkyne cycloaddition reaction and allowing for the identification of active microbial cells. Following the tagging with AHA, CY5, a far-red fluorescent dye, is used for cell sorting through Fluorescence-Activated Cell Sorting (FACS). CY5 binds specifically to the azide groups in AHA-tagged proteins. Its strong fluorescence and stability make it well-suited for high-resolution detection. In FACS, CY5 is excited by lasers, and its fluorescence emission is captured to distinguish cells based on their fluorescence intensity [61], [62], [63].

This approach enables the isolation of AHA-tagged, metabolically active cells from the complex microbial communities in the gut. By providing more accurate data, BONCAT-FACS improves the investigation of functional interactions and roles of different microbes within the microbiome with more accuracy.

The subsequent sections will detail the application of BONCAT-FACS along with other complementary techniques used in this study.

1.5.2 Raman Microspectroscopy

Raman microspectroscopy is a potent analytical method that provides molecular information, making it particularly valuable for studying complex biological samples in microscopic levels [64]. It does not need any staining or labeling for the analysis, hence this non-destructive method offers the ability to map and characterize microbial communities with high spatial resolution, providing insights into their biochemical composition and interactions within their environment [65].

This confocal microscope uses laser light to probe the molecular composition of a sample. When a laser is pointed at a sample, the majority part either gets absorbed or flows through without interaction, while the sample's molecules scatter some. Typically, the scattered light preserves the equal level of energy as the incident light, a process known as Rayleigh scattering. Nevertheless, a minor part of this light[[experiences energy change, resulting in

a shift in wavelength that is called Raman scattering. In Raman scattering, two types of shifts can occur: Stokes and anti-Stokes. When the scattered light exhibits lower energy than the incident one, Stokes scattering appears, indicating that the molecule absorbs some energy. In contrast, anti-Stokes scattering occurs when the scattered light shows higher energy than the incident light, meaning the molecule started from an excited state and lost some energy. Raman microscopy primarily measures the Stokes scattering because of the greater number of molecules in their base state at any given time. The obtained Raman spectrum serves as the sample's distinct fingerprint, showing several distinct bands that correspond to the specific vibrations of the molecules within the sample. These bands can be used to identify various chemical bonds and compounds within the sample, even in complex systems like microbial cells. Heavier atoms in the molecules cause a shift in the Raman bands, which can be used to have better understandings of the molecular structures. These shifts and intensities are the markers to identify the composition and structure of the sample at a molecular level. The vibrational spectra of different cellular components, such as lipids, proteins, nucleic acids, and carbohydrates. This technique enables the differentiation of microbial states due to nutrient utilization, response to environmental changes, or microbial interactions [64], [66]. This capability is particularly useful in understanding the gut microbiome's diversity and dynamic nature, where traditional methods may fall short.

Applying Raman microspectroscopy with other techniques such as FISH, stable isotope labeling, and optical tweezers, gives this opportunity to study complex microbial populations in a culture-independent manner [67], [68], [69].

Deuterium oxide (D_2O), heavy water, has been shown the potential for stable isotope labeling in Raman microscopy for analyzing the physiological states of the microbes[70], [71]. D_2O is a readily available and cost-effective substrate that can be used up to 50% without disturbing the growth and activity of the microbial cells [71]. In fatty acid biosynthesis, water-derived hydrogen atoms are migrated to NAD(P) during its reduction, they are subsequently integrated into lipids. When heavy water is present, deuterium (D) replaces the regular hydrogen in these processes [72]. These properties of D_2O are particularly well-suited to Raman spectrometry because once bacteria incorporate heavy

water into their biomass, a distinct peak corresponding to the C-D (carbon-deuterium) bond appears in the Raman spectrum. This peak is observed in the 2040-2300 cm^{-1} range, a region free of other peaks in typical cell spectra, making it easily distinguishable. Simultaneously, the typical C-H bond peak (2800-3100 cm^{-1}) diminishes as deuterium is increasingly incorporated into the microbial biomass. Since only active cells take up D_2O and incorporate it into their structures, the %CD can be calculated to represent the proportion of metabolically active cells within the entire microbial community [71].

1.5.3 Raman Activated Cell Sorting (RACS)

Raman Activated Cell Sorting (RACS) is an advanced technique developed by Lee and colleagues for isolating active single cells with high precision. This automated optofluidic method sorts selectively labeled single cells based on their activity and biochemical properties within various microbial samples. [69]. The system can accurately analyze up to 500 cells per hour, achieving a high accuracy rate of 98.3 ± 1.7%. RACS offers a potential solution for closing the gap between the genomic content and the functional characteristics of individual microbial cells. RACS combines multiple cutting-edge techniques to enable the precise cell sorting based on their Raman spectra; confocal Raman microspectroscopy, stable isotope probing, optical tweezers, microfluidics, and an in-house developed software platform for automation. The sorting process begins by flowing each sample into a microfluidic device at a steady rate. Random single cells are then captured and analyzed based on their Raman spectrum using optical tweezers at a focused spot. As described before, incorporating deuterium into active cell molecules changes the Raman spectra, If the system detects a shift from C-H to C-D, the stage moves automatically, and the cells are sorted into the collection outlet. In case the system does not recognize any deuterium-labeling status in Raman spectra, the sample flows to the waste outlet. This automated procedure ensures that only cells with the desired biochemical signatures are collected.

Two essential parameters in this system, P_C and P_L, are used for the real-time identification and sorting of target cells. The calculation of P_C is based on the comparison of Raman signal intensities in specific spectral regions between 1620 and 1670 cm^{-1}, denoted as $I_{1620-1670}$, with the integrated intensity of a reference fluid system within the same spectral range, denoted as $I_{fluid,1620-1670}$, providing a quantitative measure to confirm cell capture ($P_C=\frac{I_{1620-1670}}{Ifluid_{,1620-1670}}$). When optical tweezers capture a cell, the Raman intensity within the detection region increases significantly due to the laser interacting with the biological material of the cell, which scatters light and produces a Raman signal. The PC index quantifies this change in intensity, allowing the system to recognize automatically that a cell has been captured. The labeling index (P_L) is used to differentiate between D_2O labeled and unlabeled cells. The P_L index tracks the intensity of the characteristic C–D peak, allowing the system to automatically identify and sort cells labeled with deuterium. P_L is calculated by comparing the integrated Raman intensity in the spectral region between 2040 and 2300 cm^{-1}, denoted as $I_{2040-2300}$, which corresponds to the C–D peak of deuterium-labeled cells, with the integrated intensity in a nearby spectral region between 1850 and 1900 cm^{-1}, denoted as $I_{1850-1900}$, which serves as a baseline or reference for non-labeled cells ($P_L=\frac{I_{2040-2300}}{I_{1850-1900}}$) [69].

1.6 Experimental Design

This study aimed to assess the prebiotic activity of arabinogalactan in 10 healthy adult stool donors. The project included different techniques (Figure 1) to identify and isolate AG utilizer bacteria in human microbiota and analyze overall bacterial composition after incubation with AG.

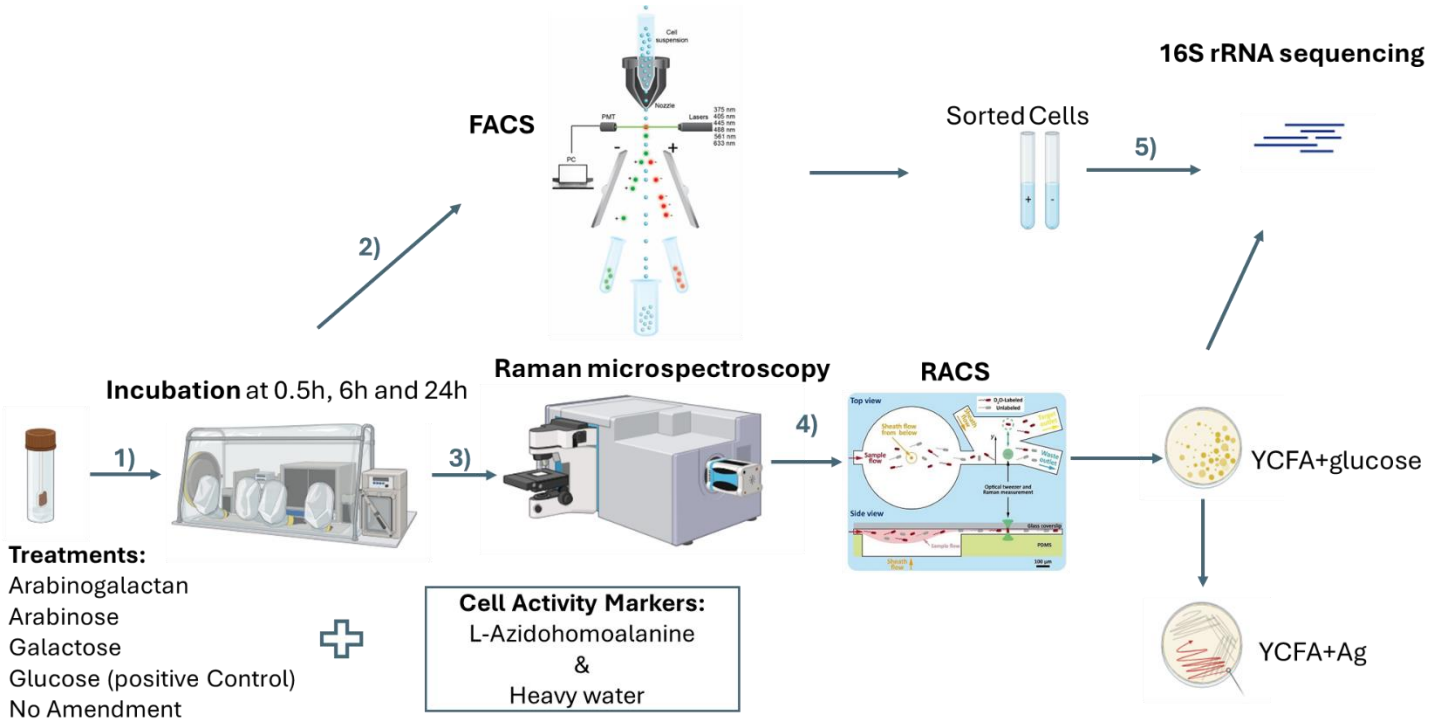

Figure 1 Experimental design of the study that included anaerobic incubation with AG, arabinose, galactose, glucose and without any amendment (1), sorting cells by flow cytometry (2), Raman microspectroscopy (3), Raman activated cell sorting (4), and 16S rRNA sequencing (5). Diagrams adapted from [73], [74] and biorender.

Chapter 2: Material and Methods

2.1 Sample collection

10 healthy volunteers (5 females and 5 males, age mean ± SD: 31.2 ± 7.18; BMI: mean ± SD: 24.37 ± 3.7) who all had omnivorous diet except donor 2 (vegetarian) were selected to collect fresh fecal samples. Exclusions from the study were those with a history of using antibiotics or probiotics/prebiotics during the previous six months, as well as those with acute or chronic intestinal diseases. The samples were obtained independently using a fecal collection tube (Sarstedt, Germany) and an anaerobic jar (Thermo Fisher Scientific, MA, USA) along with an anaerobic gas pack. The study was approved by the University of Vienna Ethics Committee (reference number 00161) and conducted in compliance with their guidelines. Written informed permission was given by the subjects prior to their enrolment in the research.

2.2 Anaerobic incubation

All incubation procedures were conducted in anaerobic tent (10% CO2, 5% H_2 and 85% N_2). Initially, 1g of fresh stool sample was suspended in 10 ml of 2x phosphate-buffered saline (PBS) and thoroughly mixed using a vortex to ensure a homogeneous suspension. Subsequently, the suspension was left for 15 minutes to facilitate the settling of large particles. Following settling, samples were pipetted from the supernatant of the diluted sample, and further diluted in a 50 ml falcon tube at a ratio of 1:10 with 2x PBS (final concentration of 1%). Compounds of arabinose, galactose, arabinogalactan, and glucose (positive control) were dissolved in 100% heavy water (D_2O) at a concentration of 4 mg/mL and sterilized using a 0.2 µm filter.

Subsequently, 5 ml of each dissolved compound was transferred into a Hungate tube. To this mixture, 5 ml of a fecal sample and 5mM of the AHA were added. As a result, the final

concentrations of sugars, D_2O, and AHA were 2 mg/mL, 50%, and 50 µM, respectively. The tubes with no compound amendment (NA) were considered as negative control. Tubes were incubated at 37 ºC for 6 and 24 hours. Samples were collected at three time points: T0.5 (in this experiment, about 30 minutes were spent to prepare the samples for incubation, hence exact time zero was not recorded, except for NA samples that the 30 minutes considered as T0), T6, and T24. AT each time point, 1ml of samples was collected for 1:1 PBS:EtOH (96%) fixation (-20), 1ml for nucleic acid extraction (stored at -80), and 1ml for making glycerol stocks (40% glycerol). In order to do metabolic analysis in the next projects, supernatants were also collected and stored at -80 (1:1 dilution in PBS and centrifuged at 14000 rpm for 10 min). In addition, a sample without any cell activity marker was prepared and fixed in EtOH as described earlier, to be used as a control in BONCAT-FACS analysis.

2.3 Sorting cells by BONCAT-FACS

2.3.1 Labeling and sample preparation

In this step, a combination of two well-known methods, BONCAT and FACS, was used to sort the BONCAT positive cells from EtOH fixed samples. Two time points, 6h and 24h, and the nutrient treatments with arabinose, galactose, and arabinogalactan, as well as, without any amendment, were selected for sorting. For this aim, samples were freshly prepared before sorting. The click labelling of chemically fixed microbial cells, facilitated by Cu(I), adapted from Hatzenpichler and colleagues, was performed as explained in the next paragraph [60].

First, 250 µL of the samples were centrifuged at 10,000 rpm at room temperature for 10 minutes. After removing the supernatant, 1 ml of 96% ethanol was added, and the mixture was vortexed. The sample was then incubated for 3 minutes at room temperature. Following incubation, the sample was centrifuged again under the same conditions to pellet it. In addition, one of the samples was washed three times with PBS without adding Cy5 alkyne dye or SYBR Green for the negative control. Meanwhile, a dye pre-mix was prepared by mixing

1.25µL of 20mM $CuSO_4$ solution (stored at 4°C), 2.50µL of 50mM THPTA (stored at -20°C), and 0.30µL of cy5 alkyne dye, allowing the mixture to react for 3 minutes at room temperature (RT) in the dark. Subsequently, this pre-mix was added to 12.5µL of 100mM aminoguanidine hydrochloride (freshly prepared), 221µL of 1x PBS and 12.5µL of 100mM sodium ascorbate (freshly prepared). The tube was inverted once, without vortexing, to mix the solutions. Then, the samples were resuspended with 80µL of this final mix and incubated at room temperature for 30 minutes in the dark and washed three times with 1x PBS by centrifuging at 8,000 rpm for 5 minutes and were washed one time with 400µL of PBS. The samples were then resuspended in 500µL of 1xPBS. Then, 3µL of SYBR Green dye (final concentration 50µM) was added as DNA indicator and incubated for 30 minutes at room temperature in the dark.

2.3.2 Sorting

As described before, Cu(I)-catalyzed click labeling was employed to tag chemically fixed microbial cells before their analysis using Fluorescence-Activated Cell Sorting (FACS). This "click chemistry" approach allows for selective reactivity between azides and alkynes, enabling efficient labeling of biomolecules and cells. In this method a terminal alkyne, conjugated with a Cy5 fluorescent dye, reacts with an azide group present in AHA, a compound used for metabolic labeling. The reaction, facilitated by copper(I) ions, results in the creation of a triazole bond between the AHA and Cy5 dye [62]. This labeling technique enables precise tagging of microbial cells and for their effective sorting based on fluorescence characteristics via FACS. In this part of the study, the aim was to sort the metabolically active cells based on their fluorescence intensity in FACS Melody instrument by using BD FACSChorus™ software.

To ensure accurate analysis and sorting of bacteria based on fluorescence and scatter properties, several preparatory steps were undertaken before initiating the sorting process (Figure 2).

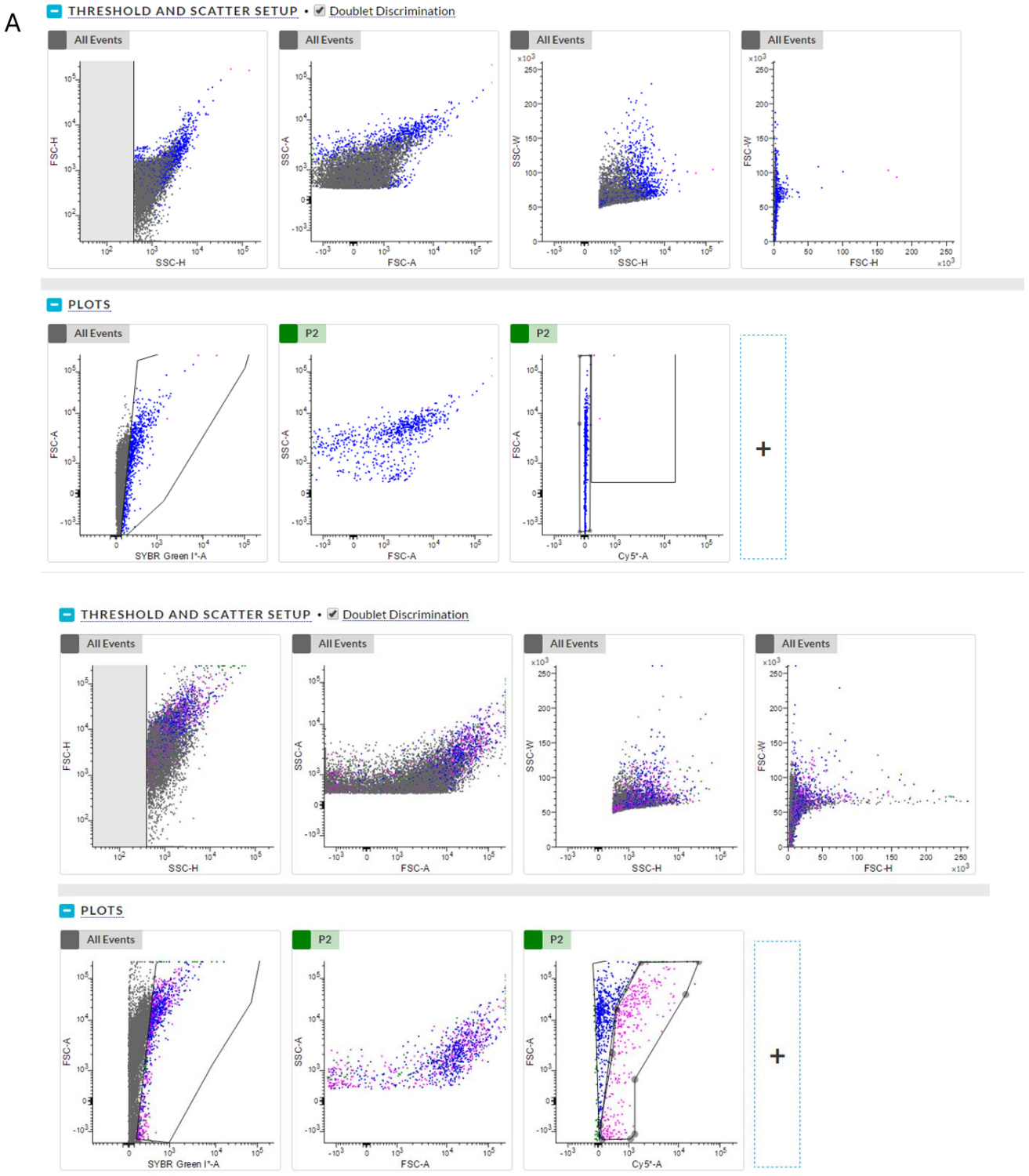

Figure 2 Gating strategy for sorting BONCAT-active cells. Shown are examples from 6 hours of incubation without amendment (A) and with arabinogalactan (B).

Baseline signals in the Forward Scatter (FSC) and Side Scatter (SSC) channels were established by running a 1xPBS through the cytometer. This crucial step was performed to set appropriate thresholds, necessary for excluding debris in subsequent analyses. Following this, a control sample, without the cell activity marker (AHA) and fluorescent dyes (Cy5 and Sybr Green), was prepared and analyzed. Debris was effectively gated out during this analysis using the scatter plot of FSC versus Sybr Green fluorescence (Fluorescein Isothiocyanate, FITC), ensuring that these non-cellular elements did not interfere with the interpretation of data. Subsequently, another sample, lacking AHA and Cy5 but including Sybr Green to stain DNA, was prepared and analyzed. This sample was utilized on an FSC versus Sybr Green (FITC) plot to identify and gate the bacterial population, thereby establishing the parent plot for further gating.

From this parent gate, filtering the population was conducted by creating a daughter plot using SSC versus FSC, focusing on cellular complexity and size. A further daughter plot was established using FSC versus Cy5 fluorescence to prepare for the specific sorting of fluorescently labeled cells. Finally, the actual sample containing AHA, Cy5, and Sybr Green was processed. Cells showing Cy5 fluorescence were identified on the FSC-Cy5 plot as labeled cells (BONCAT positive), while cells without Cy5 fluorescence but within the parent cell gate were identified as BONCAT negative. These Cy5-positive bacteria were sorted at a rate of 50,000 events per second, with the flow rate adjusted to 10, to ensure precise detection and accurate sorting.

Each step aimed to minimize background noise from the cytometer and buffer solution, and to accurately identify and sort cells according to their scatter and fluorescence characteristics. This methodical approach ensured that only the targeted cells were analyzed and sorted, minimizing contamination and enhancing the reliability of the experimental results.

The total microbial community (microcosm) and FACS sorted and unsorted cells were sent to the Joint Microbiome Facility of the Medical University of Vienna and the University of Vienna for DNA extraction and 16S rRNA amplicon sequencing (project IDs JMF-2307-05).

2.4 Raman microspectroscopy

2.4.1 Sample preparation

To detect the activity of cells by Raman, fixed samples (EtOH:PBS) that were previously incubated for 6 and 24 hours with AG and labeled with D_2O, were selected. In addition, samples with no amendments from the same time points were chosen as negative controls for each unique donor. To establish the threshold for identifying labeled cells, a control sample (incubated with glucose) without D_2O labeling was also used as a water control. From each sample, 1 μl was placed on an Al136 slide (EMF Corporation, NY, USA) covered with aluminum, and it was incubated at 30°C to allow the ethanol to evaporate. Then, the slide was submerged in cold Milli-Q water (Millipore, MA, USA and air-dried to remove the remaining salts from PBS.

2.4.2 Instrumental setup and measurement

Each day, before starting the first measurement, the Raman spectroscopy laser (532 nm) was calibrated using a silicon crystal slide to obtain a 520.5 cm^{-1} band. During the experiments, an x100 objective and a 300gr/mm diffraction grating were applied. A cell cluster was chosen for measurement, and the mapping grid was positioned over the designated area. Additionally, the delay time was set to 0 seconds, as no measurement delay was needed for this experiment. Also, binning, a statistical method of grouping multiple values of a data set, was adjusted to 1 to achieve the highest resolution spectra.

The threshold was calculated by taking the mean + 3 SD from the C-D peak percentage across 32 measurements of the water control. As a small percentage of deuterium naturally exists in water, this control was essential to determining the lowest percentage of the C-D peak needed to identify the active cells. This statistical approach ensures a robust differentiation between naturally occurring and experimentally introduced deuterium levels in the samples.

For each sample, 30-35 spectra of single cells were used to calculate the percentage of the C-D peak. Following the measurement, spectra were selected based on their resolution and the presence of characteristic peaks. A C-H peak between 2800-3100 cm^{-1} and a Phenylalanine peak near 1001 cm^{-1} indicated the presence of the cells and observation of C-D peak at the range of 2040 cm^{-1} and 2300 cm^{-1} was used as the marker for metabolically active cells [68], [71]. This part of experiment was done by Miriam Philipp.

2.5 Raman Activated Cell Sorting (RACS)

Preparation setups and the process of isolating cells by RACS was adapted from the protocol of Lee et al. 2019 [69].

2.5.1 Fabrication of microfluidic device

In the first step, current agent (Sylgard 184™, Dow corning, Michigan, USA) and base elastomer (Sylgard 184™, Dow corning, Michigan, USA) were mixed and vortexed to obtain the ratio of 10:1 and about 10g polydimethylsiloxane (PDMS). Then, PDMS was poured into a Petri dish containing a fixed master mold with pre-engineered patterns of microfluidic channels and resulted on1mm a thin layer. Air bubbles in this layer were removed using a rubber dust air blower. A 70g PDMS mixture was made again with the same ratio and poured into a clean Petri dish with about 5mm thickness to make bricks for covering the chip channels. Both dishes were baked in oven at 75ºC for at least 30 minutes to polymerize. The thin PDMS layer was carefully cut around each microfluidic device and gently peeled off the master mold with a tweezer. For the ticker PDMS layer, two bricks (5 × 10 × 5 mm^3) were cut out for each microfluidic device. The surface of the two bricks and microfluidic device (the side lacking channels) were treated by a corona treater (Electro-technic products, Illinois, USA), the two bricks were attached to inlet and outlet ports and baked at 75ºC for at least 30 minutes. Then, holes were punched in the ports using a puncher (Ø 0.75 mm, WellTech, Taiwan) allowing the sorting system tubes to be connected to the channels. In the end, the microfluidic device was placed on a high precision glass coverslip (60 x 24 x 0.17 mm, Paul

Marienfeld, Germany) by corona treater and again, was incubated in the same condition as above and after this step, the device was ready to use for sorting. Throughout these steps, forming and remaining bubbles were avoided, ensuring that the sorting process would not be disrupted.

2.5.2 Sample preparation

In this step, the glycerol stocks (-80°C) from fecal samples that were incubated with AG for 6h were selected for sorting. 150µl of samples was centrifuged at 10000 rpm for 10 minutes followed by 2 steps washing with 0.3M PBS/glycerol (centrifuging at 7000 rpm for 7 minutes). The pellet was resuspended in 500µl PBS/glycerol (0.3M) and then injected into 500µl Hamilton syringe (Hamilton, Nevada, USA). Also, the collection syringe (1ml BRAUN, Hessen, Germany) and sheath fluid syringe (Hamilton, Nevada, USA, 1ml) were filled with autoclaved 0.3M PBS/glycerol. The whole process was done under anaerobic condition in the tent and the fluids were injected carefully to avoid bubble formation in the syringes.

2.5.3 Sorting

The process was operated by two software: LabSpec6 (Horiba Scientific, France). and MATLAB 4.2. (Mathworks, USA). Before each sorting session, the system was calibrated using a silicon crystal to produce a reference band at 520 cm^{-1}. Following calibration, the three syringes were connected to tubes and chips and then to a pump holder on the microscope instrument. The system was then configured in a syringe controller (neMESYS 290 N, Cetoni, Germany) with flow rates adjusted to 2µl/min, 7µl/min, and 5µl/min for sample, sheath fluid and collection syringes, respectively. The microfluidic device's ports were connected accordingly: the sample and sheath fluid syringes were attached to the two inlet ports, and the collection syringe to one of the outlet ports for capturing labeled cells. Additionally, a chip-tube assembly was used to connect the waste channel of the microfluidic device to an Eppendorf tube to collect unlabeled cells as waste. The slide was then fixed on Raman's stage. Once the collection, sheath, and sample fluids were introduced into the channels and bubbles were eliminated, the cell capture point was focused using a 60x water immersion objective. Two lasers were employed: a Raman laser

(532 nm) for cell detection and an optical tweezer laser (1064 nm) for cell capture. After finding the focus point, the flow rates of the sample, sheath, and collection syringes were changed to 0.06µl/min, 0,25 µl/min, and -0.1 µl/min, respectively, followed by automated system calibration by MATLAB. To establish a threshold for detecting and capturing the cells, a control sample incubated with glucose for 6h (without any cell activity marker) was used to determine P_C (cell index, detection of cells by optical tweezers) and P_L (label index, detection of D2O-labeled cells by Raman). In this study, P_C and P_L values were 1.1 and 6.0, respectively. Each experimental sample was sorted for about 60-90 minutes, and the captured cells were collected into an Eppendorf tube from the collection syringe.

2.5.4 Culturing sorted cells from RACS

Immediately after sorting and to recover the sorted cells, 50μl of the collection tube was plated on YCFA-glucose in tent. In addition, 50μl of PBS/glycerol sheath fluid also was plated as negative control. Both plates were incubated at 37 °C until the colonies appeared. Then every single colony was cultured on two new plates containing YCFA-Glucose/YCFA-Ag and two broth media of YCFA-glucose/YCFA-AG. The grown bacteria in liquid medium were collected as glycerol stocks (pure cultures) and stored at -80°C.

2.6 Colony PCR of sorted cells from RACS

To identify sorted bacteria from RACS, each single colony grown on YCFA agar plates (containing glucose) was selected. Master mix (prepared as detailed in Table 1) in a UV-sterilized PCR hood and then transferred to anaerobic tent. A small part of the colonies was picked by the tip of a loop, dissolved in 50 µL of nuclease-free water and from this mixture, 1 µL was added to 49 µL of master mix. For the 16S rRNA amplification, two general bacterial primers, 616V (5'-AGA GTT TGA TYM TGG CTC AG-3') and 1492R (5'-GGT TAC CTT GTT ACG ACT T-3') were used. In the end, PCR reaction was carried out in a thermal cycler under conditions specified in Table 2.

Table 1 Components for making master mix per each colony PCR reaction

Master mix reagents	Volume (µl)
10x Green DreamTaq buffer (Thermo Fisher Scientific)	5
dNTPs 2mM (Thermo Fisher Scientific)	5
Forward primer 616V, 50µM (Thermo Fisher Scientific)	1
Reverse primer 1492R, 50µM (Thermo Fisher Scientific)	1
Dream Taq DNA Polymerase 5U/ µl (Thermo Fisher Scientific	0.5
H_2O PCR grade	36.5
Total volume	49

Table 2 PCR cycler program

PCR step	Temperature (ºC)	Time (min)	Number of cycles
Prime denaturation	95	4	1
Denaturation	95	0.5	34
Annealing	51	0.5	34
Elongation	72	1.5	34
Final elongation	72	10	1
Final hold	4	∞	1

2.6.1 Agarose gel electrophoresis and sending samples for sequencing

PCR products and GenRuler 1 kb (range of 250 bp to 10000 bp, Thermo Fisher Scientific, MA, USA) were loaded on LE agarose gel (1% in 1XTBE buffer) and GelRed was applied to visualize the DNAs. The gel electrophoresis was run about 30 mins at 120V in TBE buffer and by using Gel Doc XR+ System (BioRad Laboratories, CA, USA) images were captured. After ensuring the presence and purity of the DNAs, the samples were sent to Microsynth company for purification and 16s rRNA sequencing.

2.7 Statistical analysis

C-D peak percentage was calculated from Raman with Scattr (https://shiny.lisc.univie.ac.at/scattr/) and the representative graph was plotted in Microsoft Excel by Miriam Philipp. The ggplot2 package (v3.4.4) was used to construct the plots for the additional statistical analyses, which were all carried out using R studio software (https://www.r-project.org/, v4.3.2). At the first step, the isolated Amplicon Sequence Variants (ASVs) from BONCAT sorted/unsorted (6h and 24h), and all microcosm treatment samples in the three time points (0.5h, 6h and 24h) were filtered based on reads >=100. To evaluate if there is a significant change in ASVs per each donor, relative abundance, z-score, p.adj (adjusted by False Discovery Rate method) and enrichment factor were calculated, and results were illustrated by bubble plots. In the next step, using DESeq2 package (v1.42.1), the overall changes in ASVs, based on log2FoldChange (L2FC), for all donors were obtained and p.adj<=0.05 was set as significant threshold (taxa that were not detected 10 times in at least 4 donors, were excluded from the analysis). To assess the effects of donor, treatment, and time on microbial composition, distance-based redundancy analysis (db-RDA) was performed using the vegan package (v2.6.4), followed by the permutest function. In addition, Principal Coordinate Analysis (PCoA) from propr package (v5.0.2) was done to illustrate beta diversity and clustering ASVs.

2.8 Phylogenetic tree

To demonstrate the phylogenetic relationship among cells sorted via RACS, the process began by identifying the sequences through Sanger sequencing performed by Microsynth. The sequences were matched against the NCBI BLAST database, applying a similarity threshold of ≥96% to ensure accurate taxonomy classification. Subsequently, the sequences of all strains isolated from RACS were aligned by MUSCLE algorithm in MEGA software version 11.0.13 [75]. For the phylogenetic analysis, a tree was constructed employing the maximum likelihood method. This method included a robust bootstrap

analysis with 1000 replicates to validate the tree's branches, and then was rooted at the midpoint to provide a clear visualization of evolutionary relationships. This phylogenetic tree was carried out using the online version of IQ-TREE [76], [77]. The final visualization and refinement of the tree were achieved with the online tool iTOL [78], allowing for enhanced clarity and presentation of the phylogenetic relationships.

Chapter 3: Results

3.1 16S rRNA gene amplicon analysis of microcosm and FACS samples

This section analyzed the sequencing results from microcosm samples and FACS experiments, which included both BONCAT-positive sorted cells and BONCAT-negative unsorted cells.

The study utilized distance-based redundancy analysis (db-RDA) to assess the impact of various factors including treatment type, time points, individual donor differences, and sample type (microcosm or BONCAT positive), on the microbial populations ($p<=0.05$ considered as significant). The findings revealed that individual differences are the most significant determinants of microbiome composition across all conditions tested ($p=0.001$, Table 3). This underscored the critical importance of considering inter-individual variability in gut microbiome studies.

In assessing the entire microcosm samples, a baseline comparison of non-amended (NA) microcosm populations at time 0 with treatments involving arabinogalactan (AG), arabinose and galactose across three time points indicated significant differences ($p=0.047$). These effects were further supported when comparing the BONCAT positive fraction to inactive cells, as well as their relationship to the whole microbial community ($p=0.03$ and $p=0.004$, respectively). These findings underscored the substantial influence of the applied treatments on microbiome dynamics.

Considering the notable effect of treatments, further analyses specifically addressed the influence of arabinogalactan. AG significantly changed the microbiome composition in microcosm samples across all time points when compared to NA at time 0 ($p=0.039$). The active fractions of AG treatments also showed significant influences when contrasted with both the BONCAT positive fraction of NA samples ($p=0.030$) and the entire NA microcosm at time 0 ($p=0.05$), emphasizing AG's unique impact on microbial dynamics.

These results collectively highlighted the need to account for individual differences and specific treatment impacts, with AG showing a distinct ability to influence microbial compositions. Detailed statistical results are presented in Table 3.

Table 3 db-RDA analysis of factors influencing gut microbiome composition. This table presents comparisons used to assess the p-values association with individual differences, treatment effects, time points, and various sample types in the study.

Comparison	Significant Factors (p-value <=0.05)
All microcosm samples	Individual differences (p= 0.001)
Sugar treatments microcosm (3 time points) ~NA microcosm (0h)	Individual differences (p= 0.001) Treatment (p= 0.047)
All microcosm samples ~ BONCAT positive	Individual differences (p= 0.001) Treatment (p= 0.004) Sample type (p= 0.001)
BONCAT negative ~ BONCAT positive	Individual differences (p= 0.001) Treatment (p= 0.03) Sample type (p= 0.001)
AG treatment microcosm ~NA microcosm (0h)	Individual differences (p= 0.001) Treatment (p= 0.039)
AG BONCAT positive ~ NA BONCAT positive	Individual differences (p= 0.001) Treatment (p= 0.03) Sample type (p= 0.001)
AG BONCAT positive ~ AG microcosm (0.5h)	Individual differences (p= 0.001) Sample type (p= 0.001) Time points (p=0.004)
AG BONCAT positive ~ NA microcosm (0h)	Individual differences (p= 0.003) Treatment (p= 0.05)

Principal Component Analysis (PCA) was employed to visualize the relationships within the gut microbiome data across all microcosm samples (Figure 3). The first two principal components (PC1 and PC2) accounted for 16.93% and 13.92% of the total variance, respectively. These values reflected the multi-dimensional nature of the microbiome data due to the large number of bacterial species and their complex interactions. Although these percentages were modest, the PCA plot revealed distinct clustering patterns, predominantly influenced by donor identity. This suggested substantial inter-individual variability in gut microbiome composition. Notably, donors 1, 3, 4, and 8 clustered closely together, indicating that their microbial communities were more similar compared to others. In contrast, donors 2 and 10 were isolated from the other clusters. This isolation could have reflected the vegetarian diet of donor 2 and possibly dietary preferences or other personal factors affecting donor 10. These patterns of individual variation, which were supported by db-RDA analysis ($p=0.001$), highlighted the predominant influence of personal characteristics over dietary treatments.

Despite this variability, dietary interventions also appeared to influence the microbiome, as evidenced by slight grouping according to treatment types in the plot ($p=0.047$). However, this influence was not marked, suggesting that while dietary treatments did affect the microbiota, their impact was consistently overshadowed by the unique characteristics of each donor's microbiota.

These observed clustering patterns might also have reflected the temporal dynamics within the microbiome. Since microbial responses to dietary interventions can evolve over time, differences in sampling times across treatments might have contributed to the spread across principal components, depicting dynamic shifts in microbial populations rather than static differences.

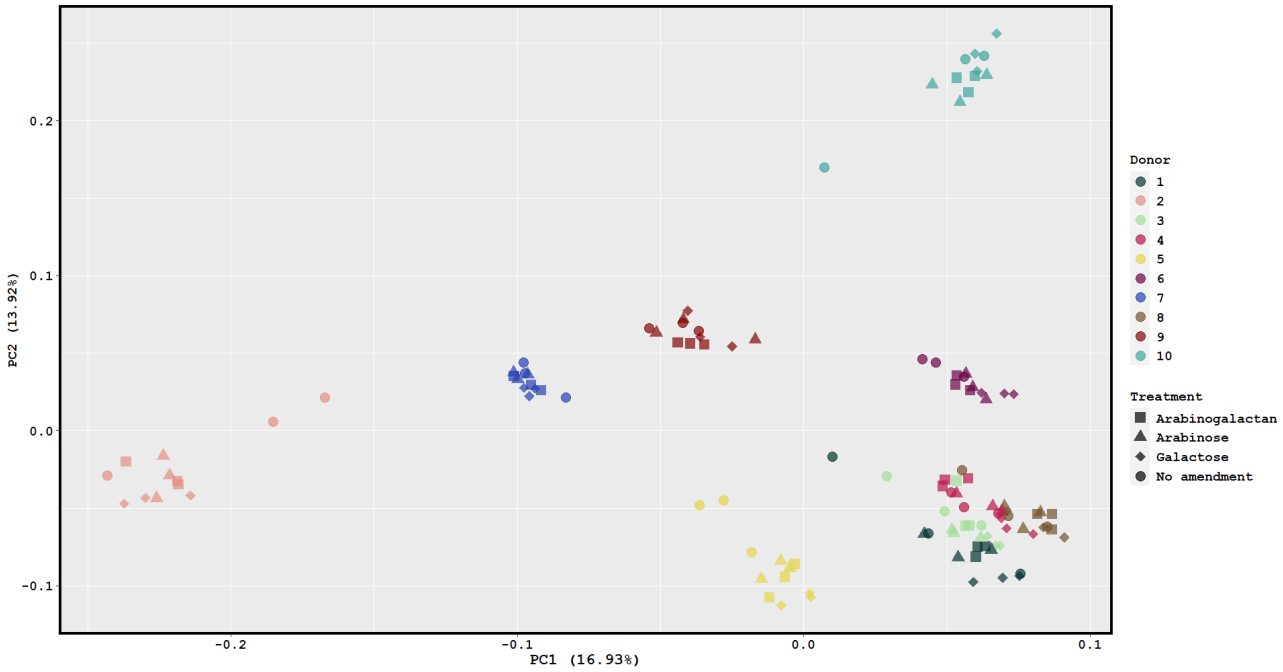

Figure 3 Principal Component Analysis (PCA) of the whole microbial community across all treatments and time points

The PCA visualization of microcosm samples and BONCAT-positive fractions illustrated key aspects of microbial community structure and metabolic activity (Figure 4). The first two principal components accounted for 16.16% and 14.46% of the variance, respectively, totaling 30.62%, indicating again the complexity of the gut microbiota. Within both sample type groups, clustering by donor was evident, underscoring the persistent influence of individual variability even within specific functional groups of microbes. This suggested that host-specific factors continued to play a crucial role in shaping the metabolically active subset of the microbiome (p=0.001).

Moreover, the plot revealed a separation between the groups, highlighting distinct microbial communities based on metabolic activity (p=0.001). The partial overlap between BONCAT-positive and microcosm samples implied that while there were differences, there was also considerable similarity between these two groups. This suggested that the metabolically active population was not entirely distinct from the broader community but rather represented a subset with some unique characteristics.

Furthermore, the treatment effects, as supported by the db-RDA analysis (p=0.004), demonstrated that dietary interventions could indeed induce shifts in microbial communities. However, these effects were relatively subtle compared to the strong impact of individual differences.

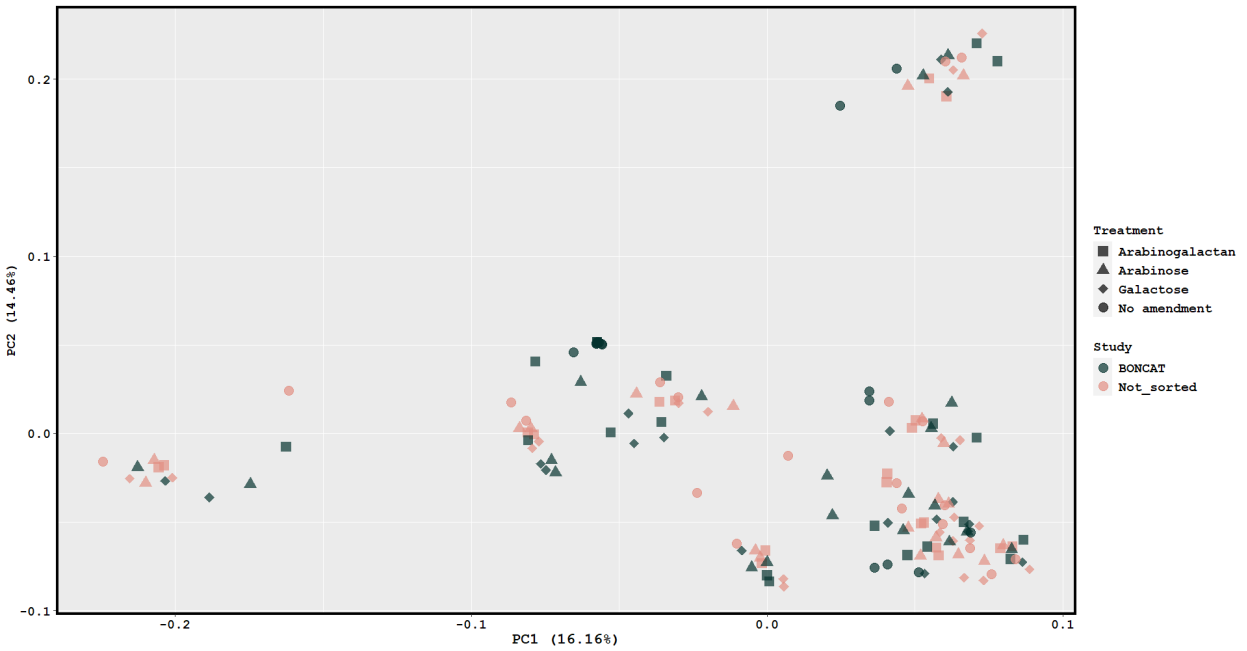

Figure 4 Principal Component Analysis (PCA) of comparing the whole microbial community and BONCAT positive fraction of FACS across the all time points.

To closely examine the impact of AG treatment on bacterial populations, a visualization based on the phylum taxonomic level was done (Figure 5). This analysis compared AG treatments of microcosm samples across all time points with no amendment samples at 0 hours, reflecting significant results previously established (p=0.039 for treatment; p=0.001 for donor differences).

At the reference time point (0 and 0.5 hours), the microbial composition showed similar patterns across individuals, with some differences potentially attributable to the short AG incubation at 0.5 hours. *Bacteroidetes* and *Firmicutes* emerged as the dominant phyla across all samples, consistent with typical gut microbiome profiles. However, notable donor-specific variations were observed:

- Donors 6, 8, and 10 exhibited a higher presence of *Verrucomicrobia*.
- Donor 3 showed a lower abundance of *Firmicutes* compared to other donors.
- Actinobacteria was detected at very low levels in donor 6.

Over the 24h incubation period with AG, an increase in *Actinobacteria* was observed in almost all samples with notable rises in donors 2, 3, and 9, suggesting a positive response to AG over time. Simultaneously, there was an elevation in *Firmicutes* in donors 2 and 3, and a modest rise in donor 4, which was accompanied by a reduction in *Bacteroidetes*. Conversely, donors 5, 6 and 8 experienced growths of *Bacteroidetes* and depletion of *Firmicutes* over time.

In donors 1 and 7, *Firmicutes* and *Bacteroidetes* remained relatively unchanged. Although there was an initial boost in *Bacteroidetes* and a corresponding decline in *Firmicutes* in donors 9 and 10 at 6 hours, these changes were not maintained by the 24h mark.

The level of *Proteobacteria* remained relatively stable across the timeframe, with a notable enrichment in donor 9 and minor depletion in donor 1.

Verrucomicrobia experienced a temporary rise after 6 hours in donors 6 and 7. Moreover, after 24 hours, it showed enrichment in donor 8 and a decreased presence in donor 10.

These observations highlighted the complex and individualized responses of gut microbiota to AG treatment. The significant differences between donors and treatments supported the notion that both factors, especially the hosts, played crucial roles in shaping microbial community structure.

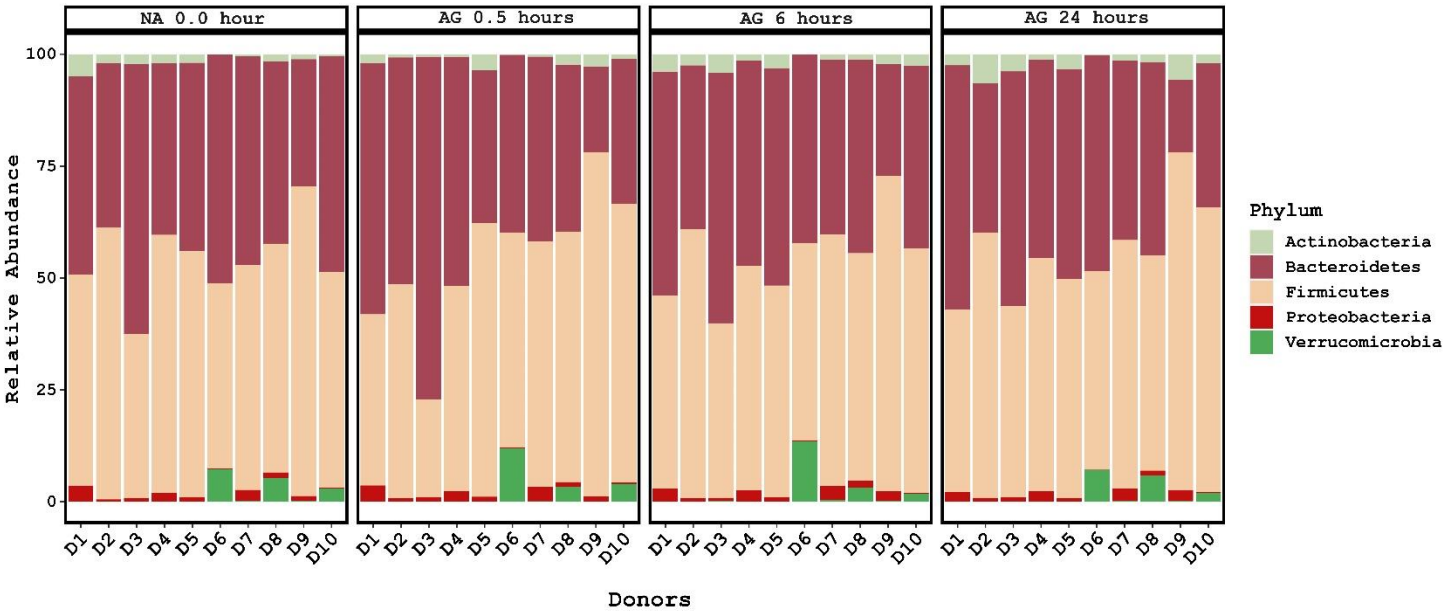

Figure 5 Phylum level bacterial composition of microcosm samples during arabinogalactan (AG) treatment of all time points, compared with no amendment (NA) samples at 0.0h.

3.2 16S rRNA amplicon analysis of microcosm and FACS samples at genus level

To gain a comprehensive view of which ASVs specifically changed with AG treatment across all donors, log2FoldChange was calculated, with significance set at adjusted p-values (p.adj) of ≤0.05. In the comparison of active cells (BONCAT positive) to the inactive fraction (BONCAT negative), *Paraprevotella* was the only genus that demonstrated consistent and significant change across all donors after both 6 (L2FC=1.9) and 24 (L2FC=1.9) of incubation with AG (p.adj=0.002 for both time points).

Furthermore, when comparing AG supplement of the microcosm samples at 6 and 24 hours relative to 0.5 hours of the same treatment, four genera were found to be significantly enriched over 24 hours (Figure 6). These included *Anaerobutyricum* (L2FC= 1.36, p.adj ≤ 0.031), *Anaerostipes* (L2FC= 1.44, p.adj ≤ 0.030), *Bifidobacterium* (L2FC= 0.79, p.adj ≤ 0.042) and *Collinsella* (L2FC= 1.09, p.adj ≤ 0.031).

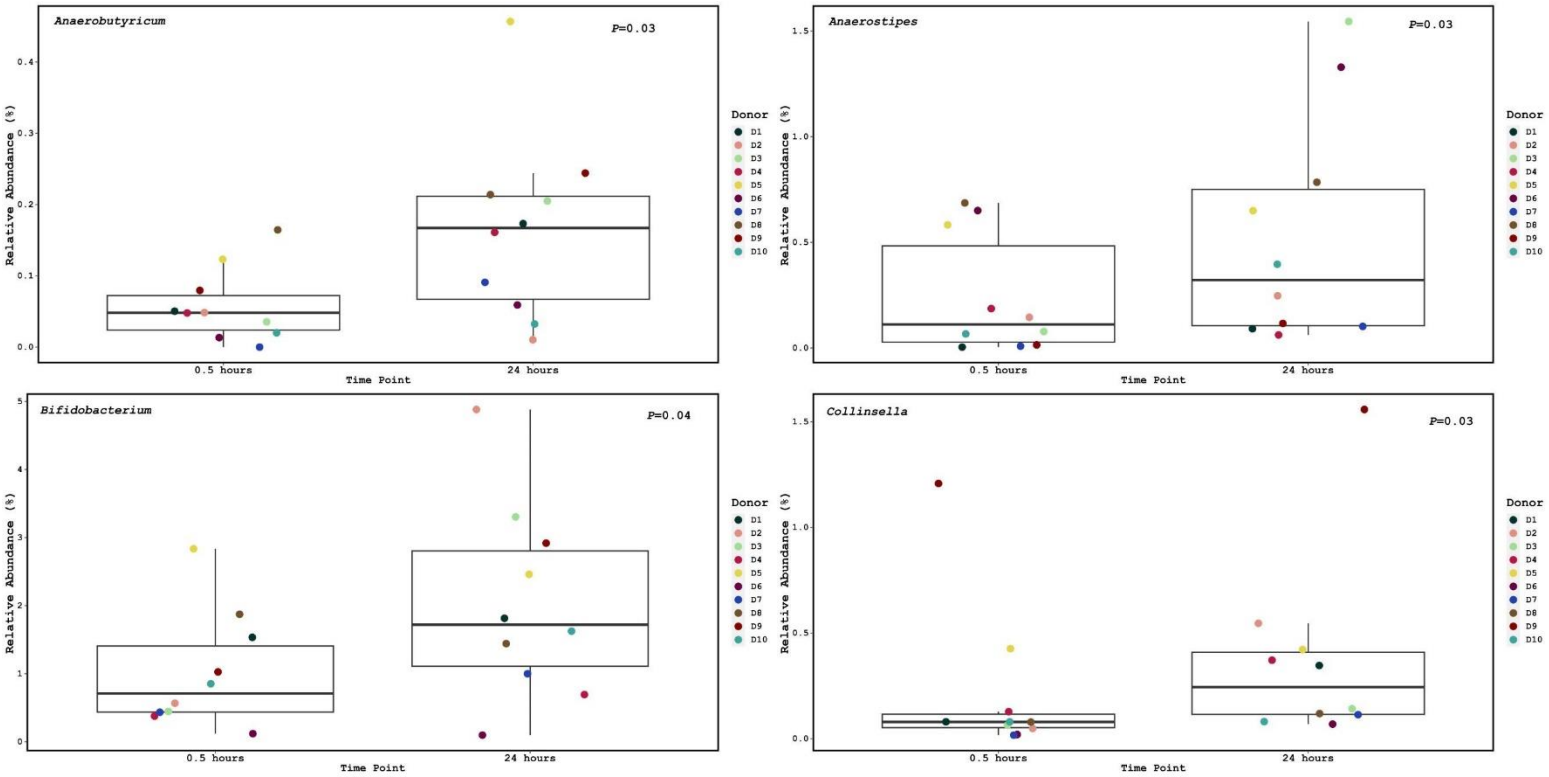

Figure 6 Based on DESeq2 analysis, significant growth of *Anaerobutyricum*, *Anaerostipes*, *Bifidobacterium*, and *Collinsella* was observed after 24 hours of incubation with arabinogalactan, compared to microcosm samples at 0.5 hours under the same treatment.

Given the notable effect of inter-individual variability on bacterial composition, as previously identified, further analyses were conducted to explore the varied responses of microbial populations to AG treatment across different donors. These analyses focused on responses at the genus level within both microcosm and BONCAT-positive fractions, enabling a detailed examination of microbial dynamics. To achieve this, the enrichment factors were calculated using z-scores and the relative abundance of ASVs with significant changes determined at p.adj ≤ 0.05. The results of these analyses were visualized for each sample type (Figure 7-10). In the plots, treatments with arabinose and galactose—breakdown products of arabinogalactan—along with a no amendment control, were included for a comprehensive comparison.

In the no-amendment samples (negative control) across the four graphs, the majority of genera were either entirely absent or exhibited very low abundance, indicating minimal

microbial activity under these conditions. However, despite the overall scarcity, the growth of some taxa, such as *Alistipes*, *Bacteroides, Lachnospira* and *Ruminococcus* in microcosm samples, and *Agathobacter*, *Dorea*, *Roseburia* and *Unclassified Ruminococcaceae* in BONCAT-FACS samples was still observed. These limited enrichments were likely attributed to residual nutrients present in the samples, which provided a minimal substrate for growth. Alternatively, this could suggest that certain species possess a competitive advantage in nutrient-limited environments, allowing them to thrive under these challenging conditions. These observed activities may reflect basal microbial functions, where select species maintain essential metabolic processes even in the absence of added nutrients.

3.2.1 Microcosm samples

In the whole community at the 6h time point relative to 0.5h, *Phocaeicola* emerged as the most abundant taxon, followed closely by *Bacteroides*, across the three treatments: AG, arabinose, and galactose (Figure 7).

In the microcosm samples, despite the inter-individual variability, several genera exhibited consistent significant enrichment among some donors. Specifically, 6h incubation with AG resulted in notable increases of unclassified *Lachnospiraceae*, *Ruminococcus*, *Phocaeicola*, *Mediterraneibacter*, *Fusicatenibacter*, *Collinsella*, *Blautia*, and *Bifidobacterium* in multiple, though not all, donors. Interestingly, *Lactococcus* and *Faecalibacillus* were exclusively boosted with the AG treatment. *Agathobacter* and *Dorea* displayed elevated levels in multiple donors with AG, with occasional instances noted in one donor each under arabinose and galactose treatments, respectively.

For other treatments, arabinose led to a prominent rise in *Coprococcus*, while galactose significantly fostered growth in *Sutterella*, *Phascolarctobacterium*, *Parabacteroides*, and *Kineothrix*. In addition, *Faecalibacterium* and *Lachnospira* demonstrated higher enrichment in both arabinose and galactose treatments compared to AG.

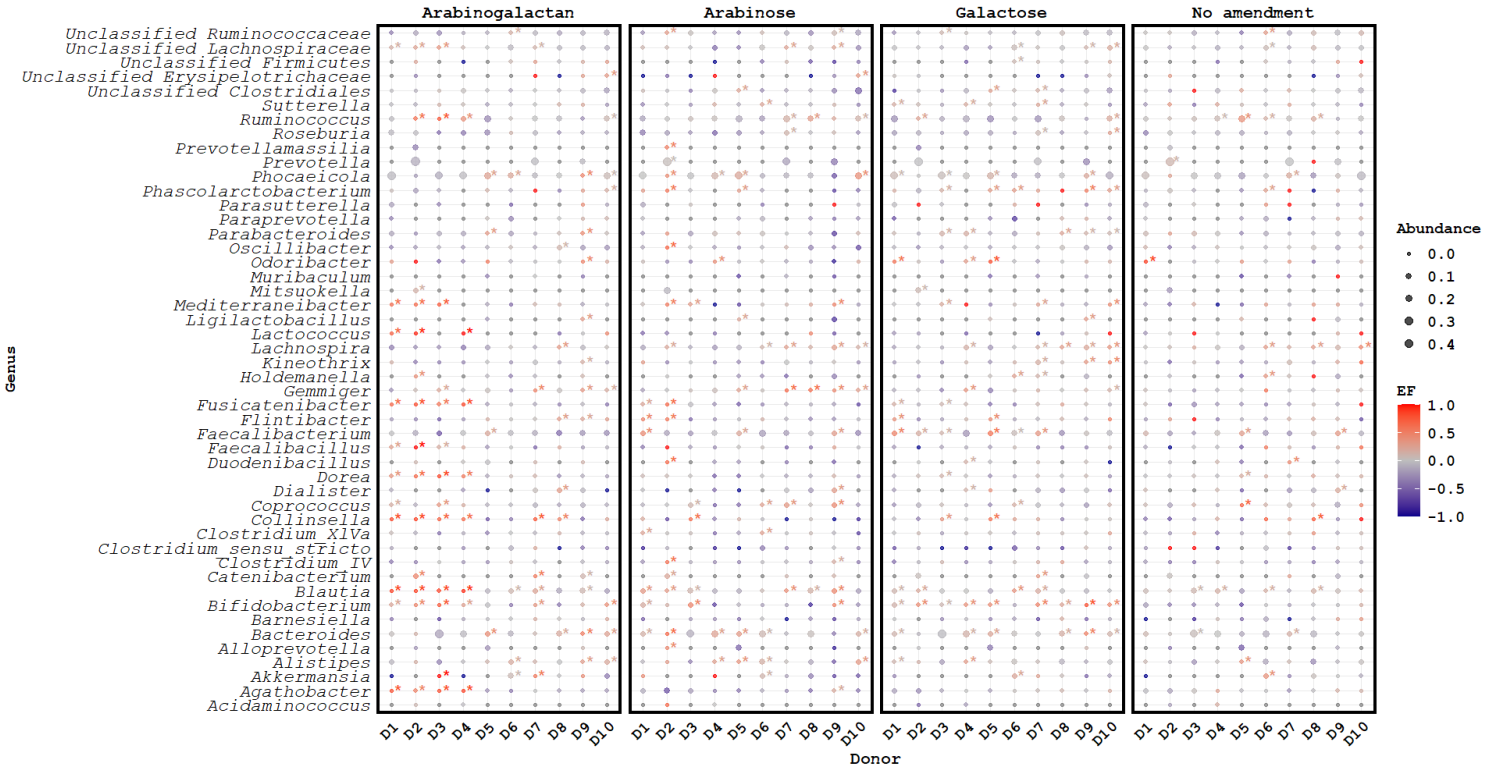

Figure 7 Genus level enrichment in microcosm samples after 6h incubation with different amendments. Bubble size, EF and asterisks indicate the relative abundance, enrichment factor, and significant enrichment (p.adj<=0.05 adjusted by False Discovery Rate method), respectively.

The whole community of 24h exhibited greater bacterial abundance and enriched genera across participants in comparison to 6h (Figure 8). While arabinose and galactose treatments maintained similar patterns of abundant taxa, AG treatment led to a more pronounced increase in *Bacteroides* compared to *Phocaeicola* relative to the 6h time point. Significant enrichment of *Bacteroides* was observed in most donors, with the exception of donors 3 and 4. However, similar to the 6h, these participants showed higher abundance of this genus among the others. Moreover, consistent and significant increases were maintained across several donors for *Ruminococcus, Mediterraneibacter*, *Fusicatenibacter*, *Dorea*, *Blautia*, *Bifidobacterium*, *Bacteroides* and *Agathobacter* under AG treatment.

The 24h incubation unveiled some shifts in microbial abundance patterns across supplements. For instance, *Phascolarctobacterium*, which showed significant changes only

in one donor at 6h with AG treatment, demonstrated a delayed response and became notably enriched in donors 1, 5, 7, and 9. Similarly, *Oscillibacter, Sutterella,* and *Lachnospira*, with increased presence in more donors at this time point. In addition, *Agathobacter* and *Lactococcus* showed exclusive elevated levels in AG treatment.

Consistent with the 6h results, *Collinsella* continued to affect more donors in AG compared to arabinose and galactose amendments. In contrast, these two sugars led to increased levels of unclassified *Firmicutes* and *Clostridium*_XlVa in some donors. Notably, *Acidaminococcus* showed significant growth in specific donors (2 and 4) during arabinose and galactose treatments, as well as in donor 2 for AG treatment, a pattern that was not observed in 6h.

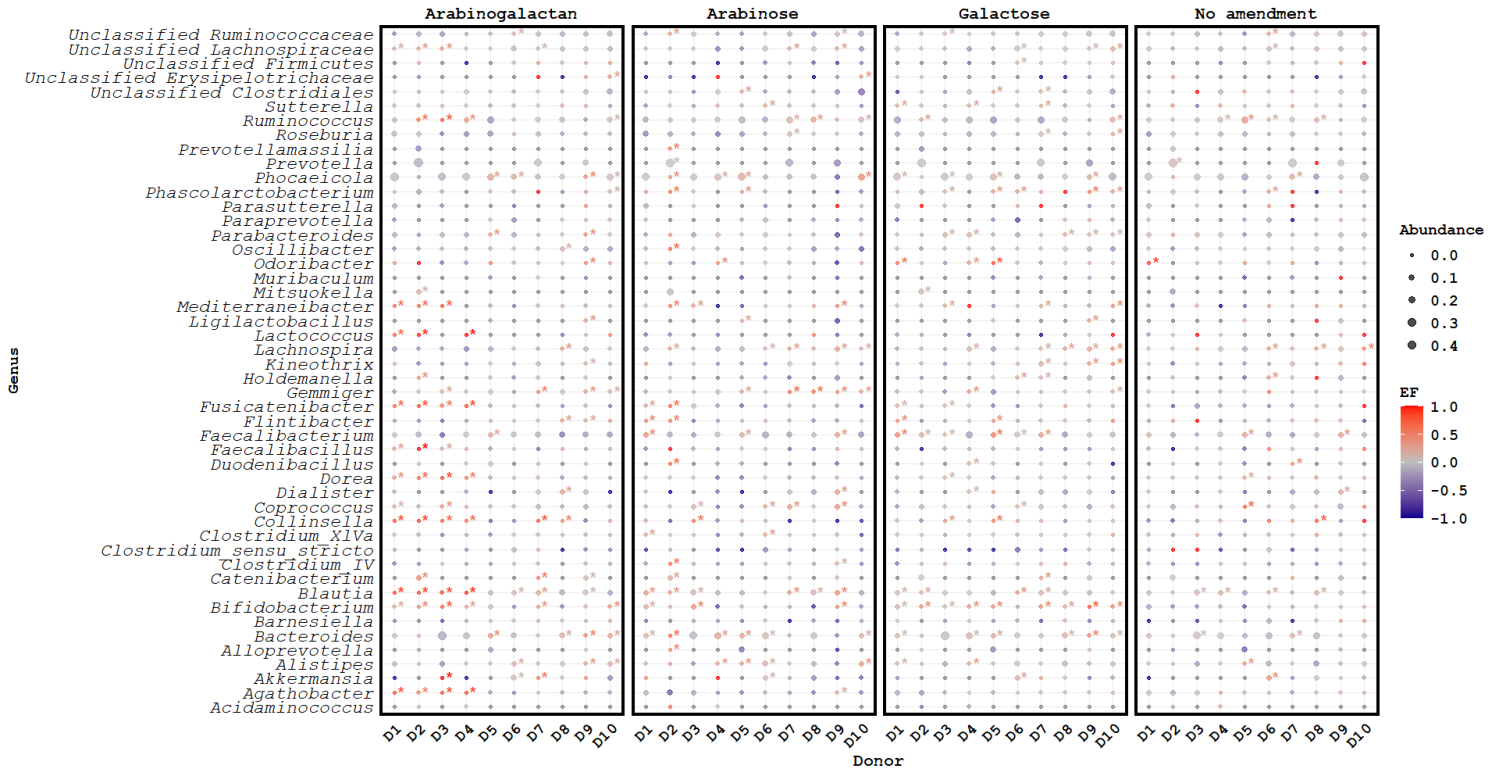

Figure 8 Genus level enrichment in microcosm samples after 24h incubation with different amendments. Bubble size, EF and asterisks indicate the relative abundance, enrichment factor, and significant enrichment (p.adj<=0.05 adjusted by False Discovery Rate method), respectively.

3.2.2 FACS samples

Analysis of the metabolically active fraction compared to inactive cells of AG treatment demonstrated significant changes in some genera (Figure 9&10). However, the effect of treatment was less pronounced in comparison to the microcosm samples. As expected from the variability underscored in earlier results, different donors exhibited distinct responses to 6h AG treatment (Figure 9). For instance, *Alistipes* showed significant growth in donors 1, 4, 6, 8, and 10, while *Bacteroides* was enriched in donors 1, 4, 5, 6, 8, and 10. *Faecalibacterium* was notably increased in donors 7, 8, and 9. Additionally, *Odoribacter* enhanced in donors 4, 6, 9, 10. *Parabacteroides* and *Phocaeicola* both exhibited significant rise in donors 4, 5, 6, 8, and 10 while *Paraprevotella* was enriched in donors 1, 5, 6, 8, and 10. And, unclassified *Lachnospiraceae* showed significant growth in donors 1, 3, 5, and 9.

Moreover, in some cases, the simpler carbohydrates, arabinose and galactose, elicited more pronounced microbial changes, particularly *Blautia*, *Bifidobacterium* and *Prevotella* were notably more increased compared to AG treatment across the donors.

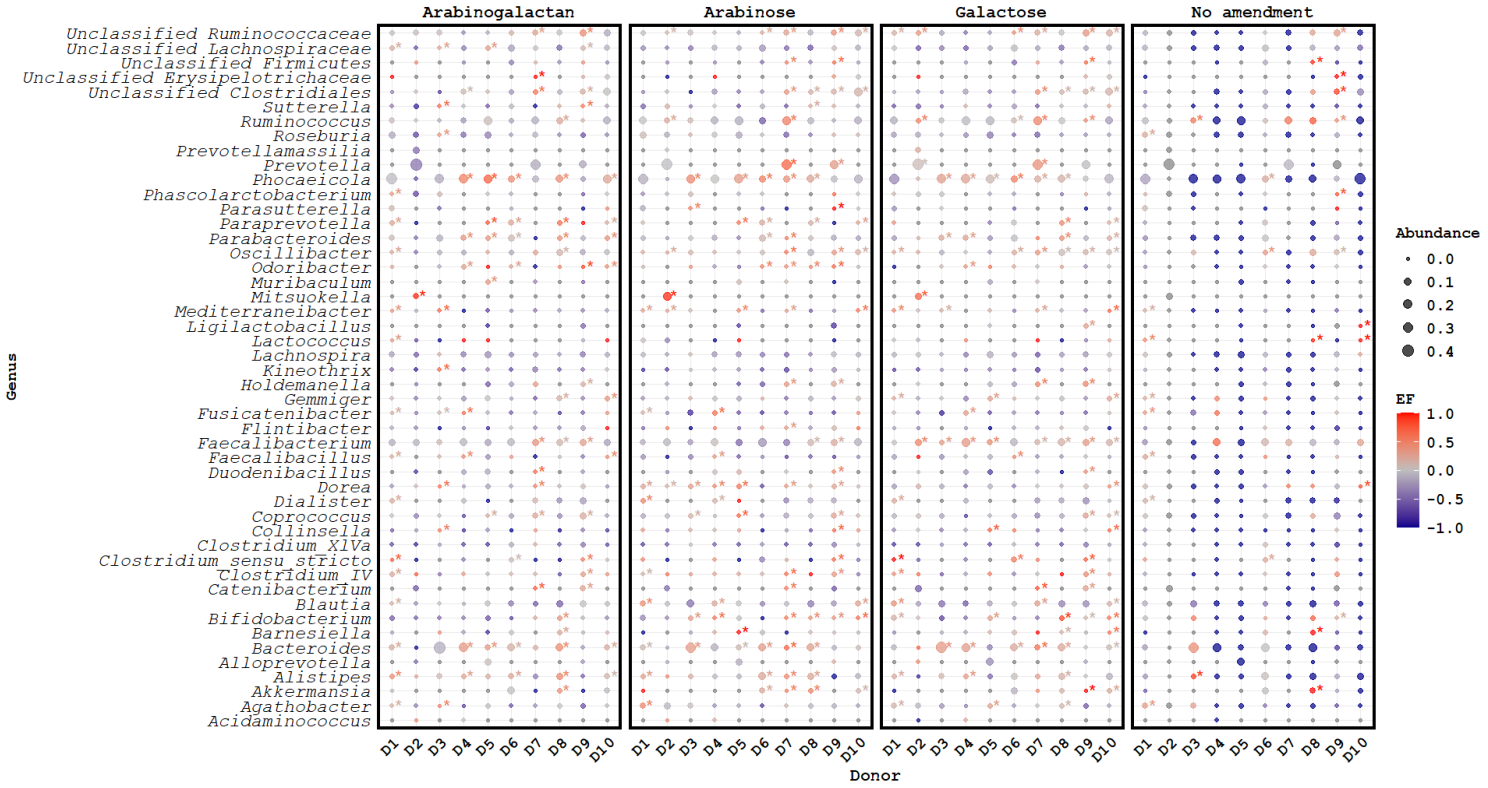

Figure 9 Genus level enrichment in metabolically active fractions (BONCAT positive-FACS) after 6h incubation with different amendments. Bubble size, EF and asterisks indicate the relative abundance, enrichment factor, and significant enrichment (p.adj<=0.05 adjusted by False Discovery Rate method), respectively.

The assessment of metabolically active cell populations after 24 hours of incubation with AG revealed a decline in the relative abundance of almost all genera. This trend was also consistent across the other two treatments (Figure 10). These findings indicated that while specific microbial shifts occurred, they were not uniformly observed at the 24h mark. This inconsistency may have stemmed from methodological challenges associated with the FACS technique utilized in this part of the experiment, as discussed in the discussion chapter.

Despite the general trend of decline, notable occurrences of significant prominence for certain minor genera were observed in specific donors in comparison the two time points. For instance, unclassified *Ruminococcaceae* was enriched in donor 3, while *Bacteroides* and unclassified *Firmicutes* were enhanced in donor 9. *Ruminococcus* showed growth in

donors 1, 5, and 7, and *Roseburia* increased in donors 1 and 4. Additionally, *Flintibacter* was raised in donor 2, and *Faecalibacterium*, *Dorea*, and *Dialister* were enriched in donor 4. *Collinsella* was noted in donors 4 and 7, and *Akkermansia* was increased in donors 7 and 10. Lastly, unclassified *Erysipelotrichaceae*, unclassified *Firmicutes*, and unclassified *Clostridiales* exhibited higher abundance in donor 10.

Supplementation of the samples with arabinose and galactose also demonstrated a similar pattern of enriched taxa, particularly for *Phocaeicola*, which showed significant increases across all treatments in most donors. However, some genera such as *Blautia* and *Bifidobacterium* presented more preference for arabinose and galactose over AG, similar to the obtained results at 6h.

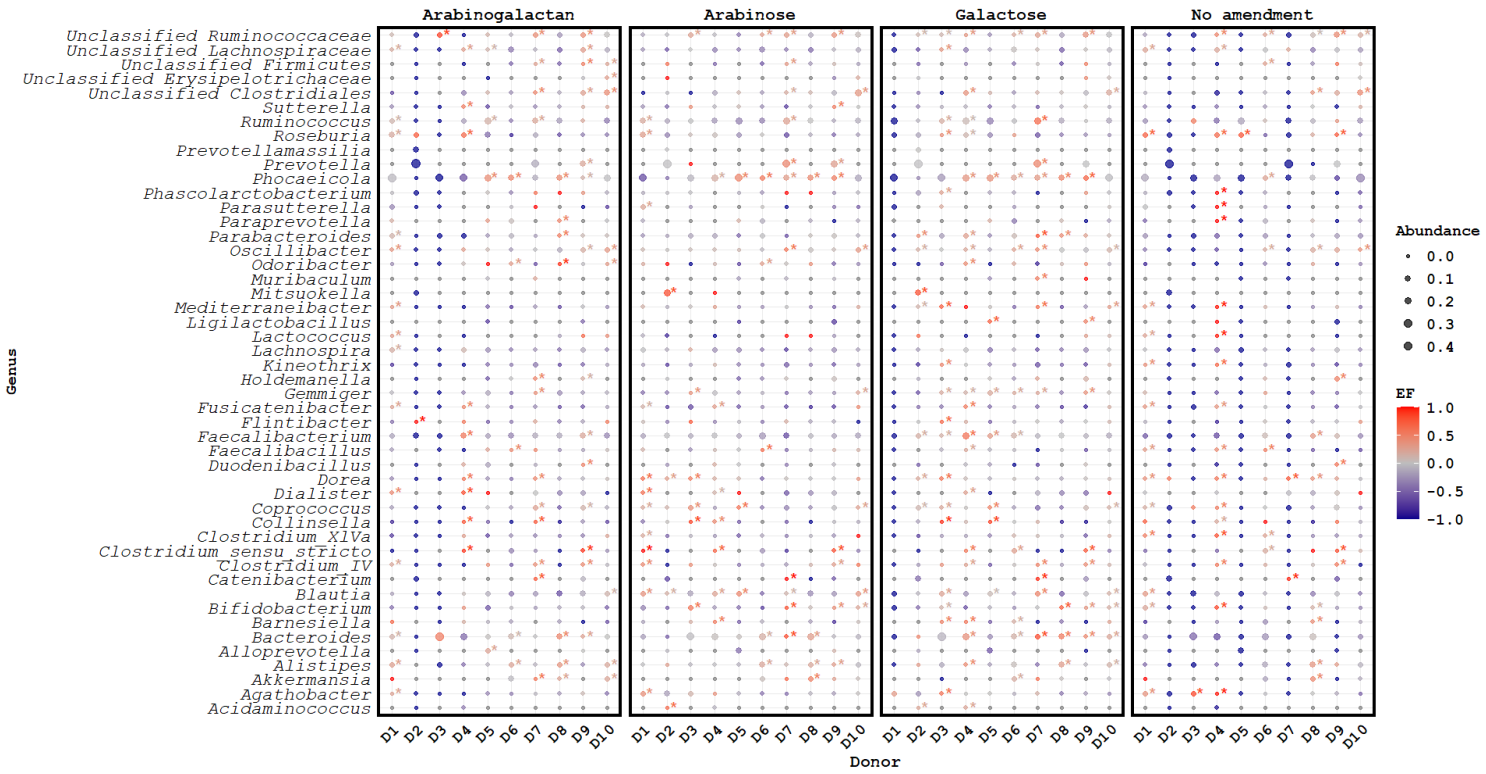

Figure 10 Genus level enrichment in metabolically active fractions (BONCAT positive-FACS) after 24h incubation with different amendments. Bubble size, EF and asterisks indicate the relative abundance, enrichment factor, and significant enrichment (p.adj<=0.05 adjusted by False Discovery Rate method), respectively.

3.3 Detected active cells by Raman microspectroscopy

Raman microspectroscopy was utilized effectively to assess the activity of bacterial populations in arabinogalactan treated samples by tracking the incorporation of deuterium (D) from D2O into cellular components, as indicated by the appearance of C-D peak in the Raman spectrum (Figure 11).

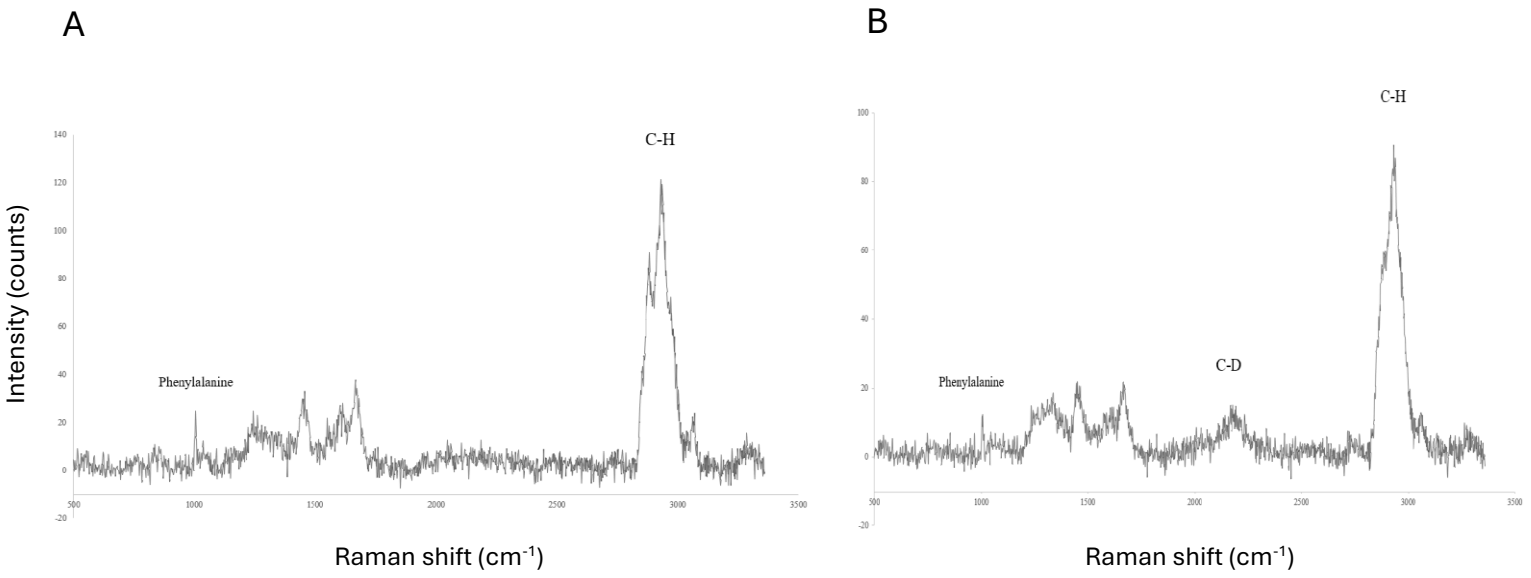

Figure 11 Raman spectrum of a bacterial cell, unlabeled (A) and labeled (B). Phenylalanine at 1001 cm^{-1} and C-H (carbon-hydrogen) peaks in the range of 2800-3100 cm^{-1} serve as cellular indicators. The C-D (carbon-deuterium) peak, ranging from 2040-2300 cm^{-1}, acts as a marker of cellular activity.

First, a threshold of 1.36% was established based on the average percentage of the C-D peak across 32 measurements of the water control (unlabeled cells), plus three times the standard deviation.

At both the 6h and 24h time points, the majority of AG treated samples displayed higher C-D peak percentages compared to controls, where activity was either below this threshold or

only slightly above (Figure 12). A notable exception was observed in donor 6 at 24 hours, who demonstrated similar deuterium levels in both treated and untreated samples.

Specifically, at the 6h mark, donor 1 exhibited the highest metabolic activity with a 7.05 ± 3.46% C-D, whereas donor 8 showed the lowest at 1.05 ± 1.21%. For no amendment samples, C-D% ranged from 0.26 ± 0.43% in donor 3 to 0.93 ± 1.20% in donor 6.

The data indicated that extended incubation generally led to marginally higher C-D peak percentages in most samples, reflecting increased metabolic activity. By 24 hours, donors 5 and 1 showed the most significant deuterium incorporation at 8.55 ± 5.26% and 8.42 ± 3.12%, respectively, with donor 8 remaining the lowest at 1.24 ± 1.07%. The highest C-D percentage among no amendment samples was recorded for donor 6 at 2.01 ± 2.91%, marking the peak across all NA samples at both time points.

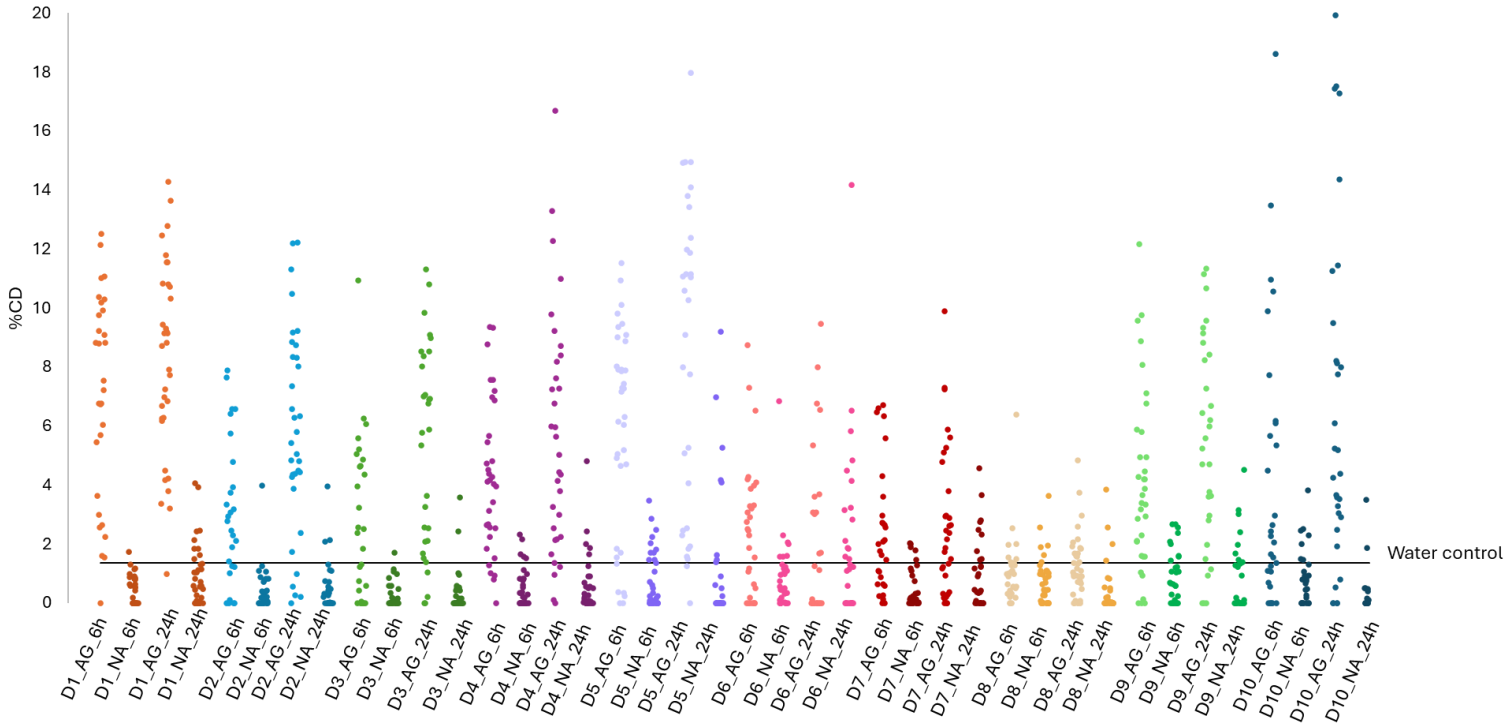

Figure 12 Percentage of C-D peaks (%CD) from Raman mapping across donor 1 (D1) through 10 (D10) following 6h and 24h incubation with arabinogalactan (AG) and no amendment (NA). The black line represents the threshold, calculated based on water control measurements, while each dot illustrates the %CD from randomly sampled cells within the mapping areas.

Additionally, the proportion of active cells from a randomly selected area in the mapping was visualized (Figure 13) and demonstrated a range from 26.66% in donor 8 to 96.67% in donor 1 at 6 hours, and from 40.0% in donor 8 to 97.06% in donor 1 at 24 hours. For clarity, only no amendment (NA) sample from donor 1 at 6 hours (3.33%) was included in the plot.

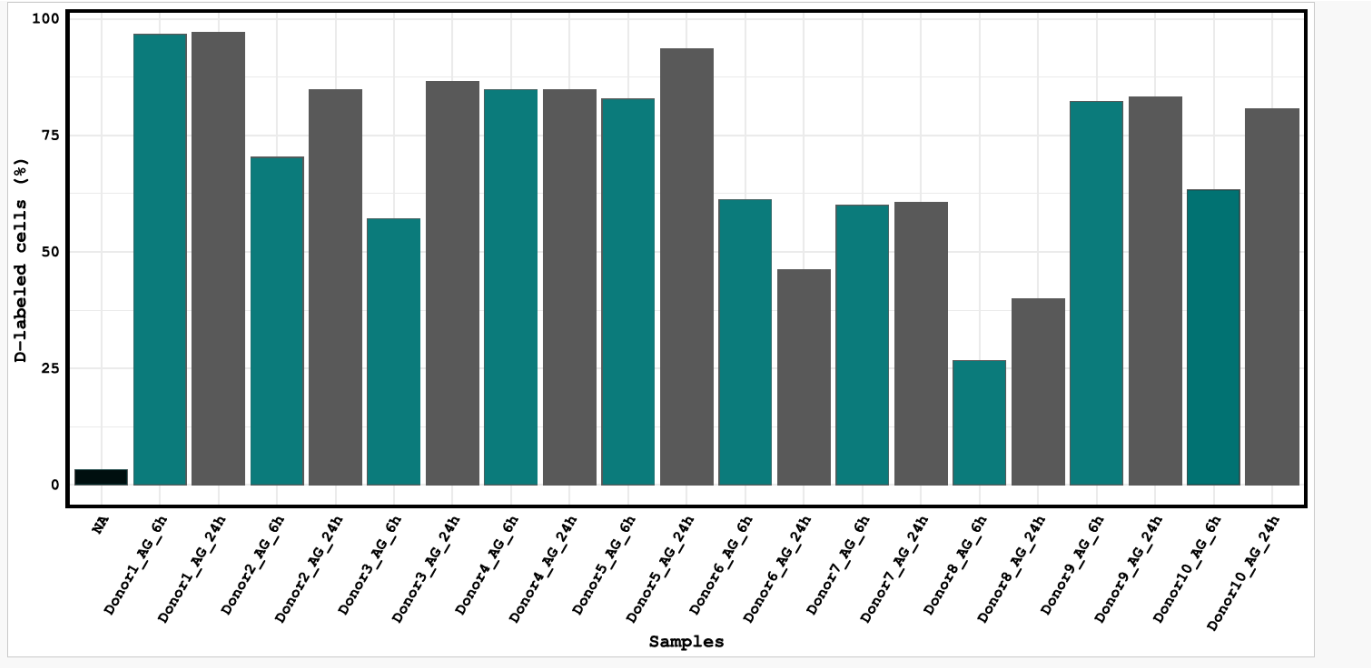

Figure 13 Percentage of active cells in each donor at 6h (blue) and 24h (grey) incubation with arabinogalactan (AG). To simplify the plot, only NA at 6h from donor 1 is presented as control.

3.4 Identified strains from Raman Activated Cell Sorting (RACS)

Following the confirmation of cellular activity via Raman microspectroscopy, which detected C-D peaks, samples from the 6h incubation with arabinogalactan were selected for sorting using RACS. This analysis indicated a varied number of isolated cells across donors, along with diverse recovery rates post-cultivation on YCFA-glucose agar medium (Table 4). Conversely, no colonies were recovered from donors 4, 6, and 9, as the sorted cells failed to grow on the media, possibly due to the isolates' sensitivity to oxygen, temperature or insufficient nutrient requirements in the medium. As a result, no further cultivable strains were obtained from these samples. In contrast, donor 10 demonstrated complete recovery rates with 27 colonies. This variable outcome highlighted the significant differences in microbial viability and cultivation success across individual donors. Additionally, certain isolates failed to recover on YCFA-AG plates, including *Collinsella aerofaciens* from donor 2 (colony 27), *Alistipes shahii* (colony 2) and *Bifidobacterium longum* (colony 5) from donor 7, and *Ruminococcus bicirculans* (single colony) from donor 8. This may be attributed to varying capabilities of the different strains.

Table 4 Number of analyzed cells by RACS, the sorting rate and their recovery on YCFA-glucose agar medium.

	Donors									
	1	2	3	4	5	6	7	8	9	10
Total analyzed cells (n)	1021	798	239	174	182	843	169	548	192	782
D-labeled cells (n)	5	28	63	7	60	25	26	40	24	27
Sorting rate (%)	0.48	3.5	26.35	4.02	32.96	2.96	15.38	7.29	12.5	3.45
Colonies recovered (n)	1	27	33	0	1	0	8	1	0	27
Recovery rate (%)	20	96.4	52.3	0	1.6	0	30.76	2.5	0	100

With this approach, 98 bacterial strains were isolated and subjected to 16S rRNA gene sequencing. BLAST analysis against the NCBI database identified 12 and 16 distinct genera and species, respectively among the isolates (Figure 14). The *Bifidobacterium longum* was the most predominant, representing 45.9% (45 out of 98) of the recovered strains, followed by *Collinsella aerofaciens*, which accounted for 26.5%. The remaining isolates were classified into the following genera: *Alistipes*, *Bacteroides*, *Catenibacterium*, *Dysosmobacter*, *Eggerthella*, *Faecalibacterium*, *Parabacteroides*, *Phascolarctobacterium*, *Phocaeicola*, and *Ruminococcus*.

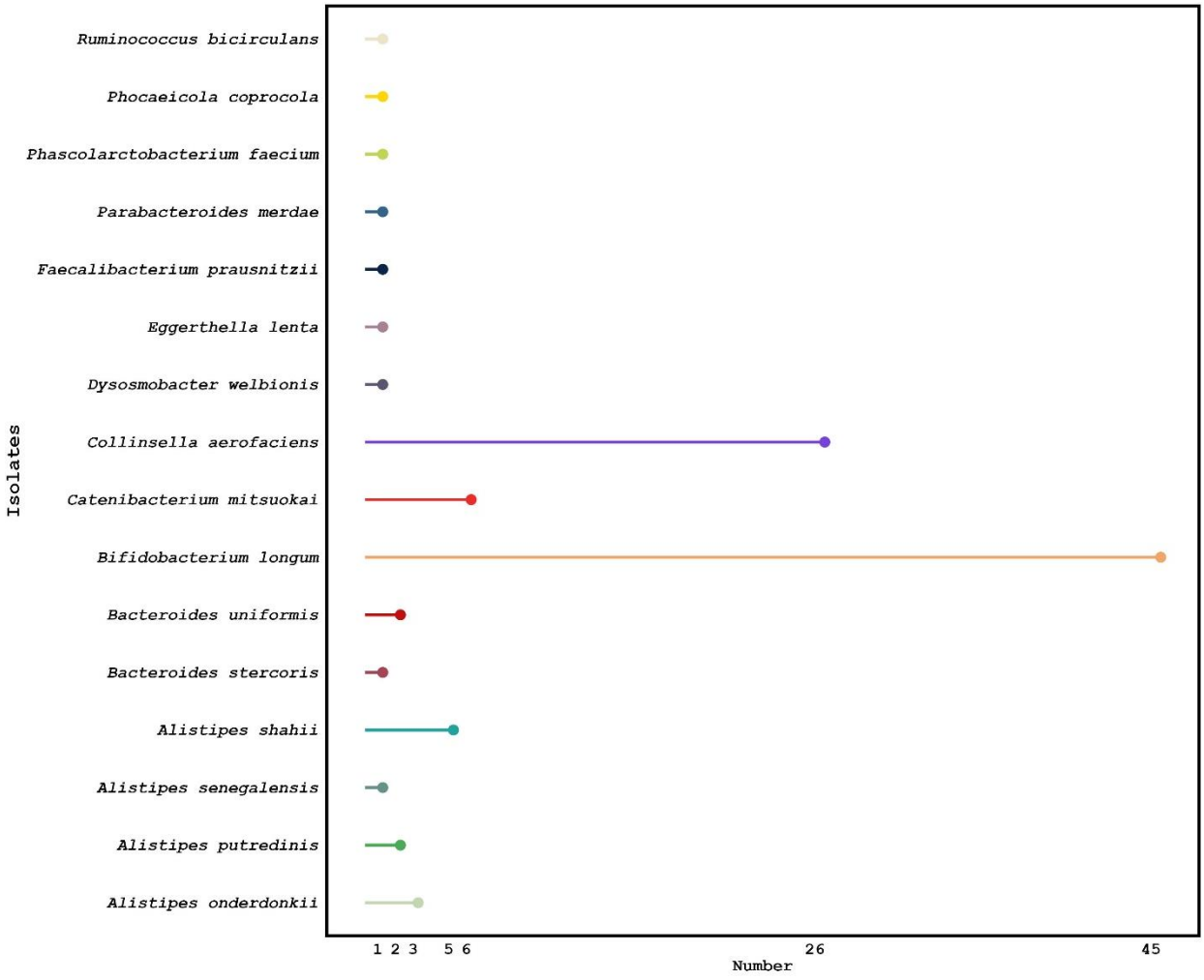

Figure 14 Identity and total recovered cells from RACS analysis across all donors.

To illustrate the relationships between the identified species, a phylogenetic tree was constructed using the online version of IQ-TREE that identified TIM2+F+I+G4 as the best-fit model based on the Bayesian Information Criterion (Figure 15). The analysis encompassed 98 isolates representing 16 unique species, which were taxonomically distributed across three major bacterial phyla: *Actinobacteria* (72 strains, 73.5%), *Bacteroidetes* (16 strains, 16.3%), and *Firmicutes* (10 strains, 10.2%). The phylogenetic tree indicated that, although not all isolates showed host-specific patterns, the majority from the same donor tended to cluster together as they share greater genetic similarity. This pattern aligned with the earlier findings, which demonstrated the significant impact of host-specific factors on shaping the composition and diversity of host bacterial composition.

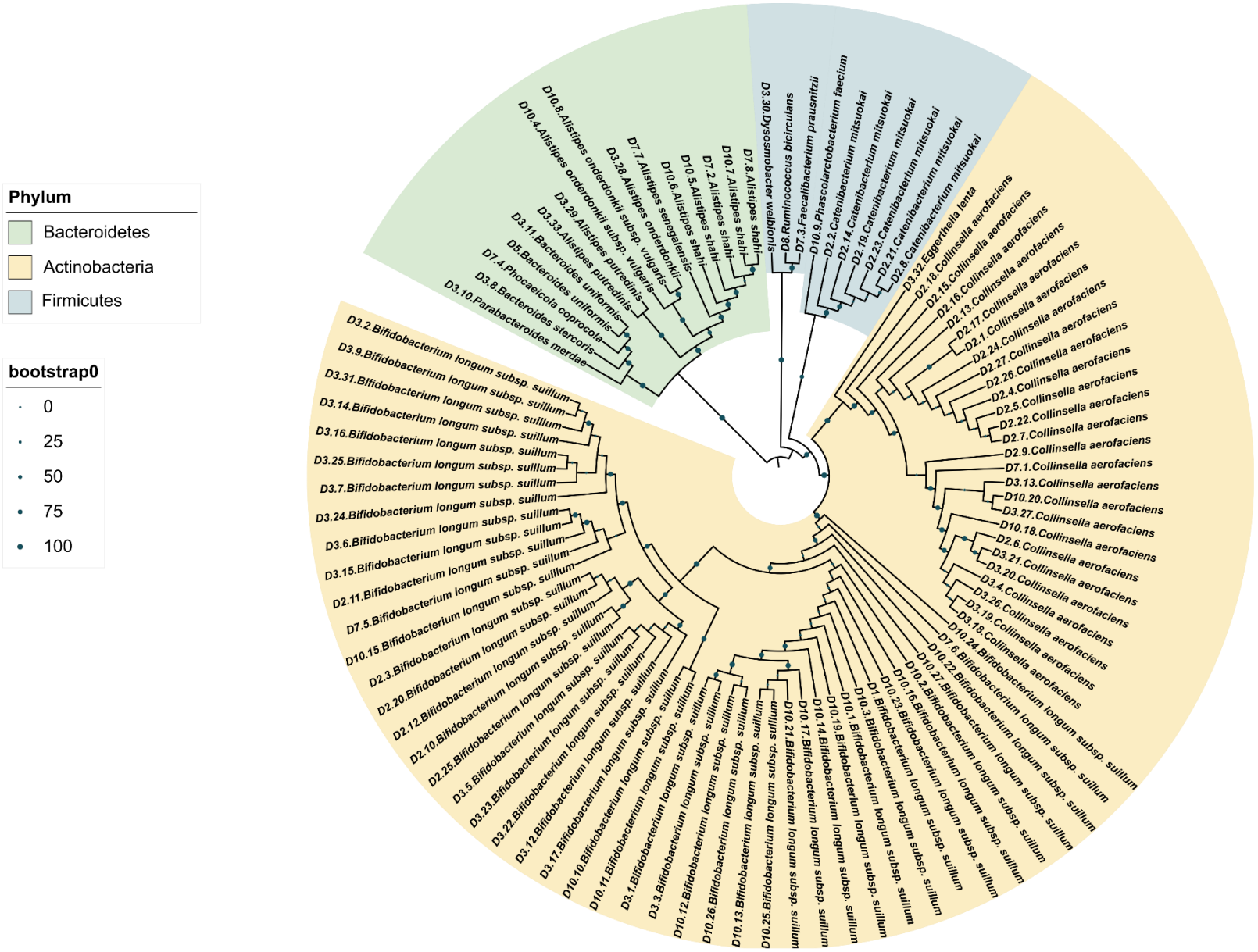

Figure 15 Phylogenetic relationships of 98 isolated strains from RACS technique.

The overall analysis of enriched genera from the microcosm and BONCA-FACS samples, and recovered isolates from RACS revealed that *Alistipes*, *Bacteroides*, *Bifidobacterium*, *Catenibacterium*, *Collinsella*, *Faecalibacterium*, *Oscillibacter*, *Parabacteroides*, *Phocaeicola*, and *Ruminococcus* were the most consistently represented taxa across all experimental samples treated with AG (Table 5).

Table 5 Enriched genera in microcosm and BONCAT-FACS at 6h and 24h, and isolates recovered from RACS. Ag, Ara, and Gala represent arabinogalactan, arabinose, and galactose, respectively. '+' indicates positive enrichment or recovery, while '–' denotes absence. ND refers to the number of donors showing enrichment or recovery.

Conditions	Microcosm 6h/ND			Microcosm 24h/ND			BONCAT 6h/ND			BONCAT 24h/ND			RACS/ND
Treatments	**Ag**	**Ara**	**Gala**	**Ag**	**Ara**	**Gala**	**Ag**	**Ara**	**Gala**	**Ag**	**Ara**	**Gala**	**AG**
Genus													
Acidaminococcus		-		+/1	+/2	+/2		-		-	+/1	+/2	-
Agathobacter	+/4	+/1	-	+/4	-	-	+/2	+/1	+/3	+/1	+/1	+/1	-
Akkermansia	+/3	+/1	+/1	+/1	-	+/2	+/1	+/4	+/2	+/3	+/1	+/1	-
Alistipes	+/3	+/4	+/2	+/2	+/5	+/2	+/5	+/4	+/3	+/4	+/3	+/3	+/3
Alloprevotella	-	+/1	-	-	+/1	-		-		+/1	-	-	-
Anaerobutyricum	+/3	+/1	+/7	+/6	+/4	+/8	+/2	+/1	+/1	+/3	-	+/5	
Anaerostipes	+/5	+/2	+/4	+/6	+/6	+/6	+/3	+/4	+/4	+/2	+/2	+/3	
Bacteroides	+/4	+/6	+/6	+/8	+/9	+/4	+/6	+/6	+/6	+/4	+/3	+/6	+/2
Barnesiella		-			-		+/1	+/1	+/2	-	+/1	+/3	-
Bifidobacterium	+/6	+/3	+/9	+/6	+/4	+/9	+/1	+/6	+/5	-	+/4	+/4	+/5
Blautia	+/7	+/6	+/4	+/7	+/6	+/3	+/1	+/3	+/3	+/1	+/6	+/4	-
Catenibacterium	+/3	+/1	+/1	+/1	-	+/1	+/2	+/1	+/2	+/1	+/1	+/1	+/1
Clostridium IV	-	+/2	-		-		+/2	+/3	+/2	+/3	+/2	+/3	-
Clostridium XIVa	-	+/2	-	+/1	+/4	+/2		-		-	+/1	-	-
Clostridium_sensu_stricto		-			-		+/3	+/1	+/3	+/2	+/3	+/3	-
Collinsella	+/6	+/1	+/2	+/4	+/1	+/1	+/1	+/1	+/2	+/2	+/2	+/2	+/4
Coprococcus	+/2	+/4	+/1	+/3	+/4	+/2	+/3	+/3	+/2	+/2	+/4	+/4	-
Dialister	+/1	+/1	+/1	-	+/1	+/1	+/1	+/2	+/1	+/2	+/2	+/1	-
Dorea	+/4	-	+/1	+/5	+/3	+/4	+/2	+/7	+/1	+/2	+/3	+/2	-
Duodenibacillus	-	+/1	+/1	-	+/2	-	+/1	+/1	+/1	+/1	-	-	-
Eggerthella		-			-			-			-		+/1
Faecalibacillus	+/3	-	-	-	+/4	-	+/3	+/1	+/1	+/1	+/1	+/1	-
Faecalibacterium	+/1	+/3	+/6	+/1	+/2	+/3	+/3	+/2	+/8	+/2	-	+/5	+/1
Flintibacter	+/2	+/2	+/2	+/2	+/1	+/2	-	+/1	-	+/1	-	+/1	-
Fusicatenibacter	+/4	+/2	+/2	+/4	+/3	+/3	+/3	+/2	+/1	+/2	+/2	+/1	-
Gemmiger	+/4	+/5	+/2	+/4	+/1	+/4	+/2	-	+/3	+/1	+/2	+/6	-
Holdemanella	+/1	-	+/2	+/1	+/1	-	+/1	+/2	+/2	+/2	-	-	-
Kineothrix	+/1	-	+/3	+/2	+/2	+/4	+/1	-	-	-	-	+/1	-
Lachnospira	+/1	+/5	+/5	+/3	+/5	+/5		-		+/1	-	-	-
Lactococcus	+/3	-	-	+/2	-	-	+/1	-	-	+/1	-	-	-
Ligilactobacillus	+/1	+/1	+/1	-	-	+/2	-	-	+/1	-	-	+/2	-
Mediterraneibacter	+/3	+/3	+/3	+/4	+/4	+/3	+/2	+/6	+/4	+/1	-	+/4	-
Mitsuokella	+/1	-	+/1	-	-	+/1	+/1	+/1	+/1	-	+/1	+/1	-
Muribaculum		-			-		+/1	-	-	-	-	+/1	-
Odoribacter	+/1	+/1	+/3	+/1	+/1	+/1	+/4	+/4	+/1	+/3	+/1	+/1	-
Oscillibacter	+/1	+/1	-	+/3	+/4	+/2	+/2	+/4	+/6	+3	+/2	+/5	+/1
Parabacteroides	+/2	-	+/5	+/3	-	+/1	+/5	+/2	+/4	+/2	-	+/4	+/1
Paraprevotella		-			-		+/5	+/4	+/2	+/1	-	-	-
Parasutterella		-			-		-	+/2	-	-	+/1	-	-
Phascolarctobacterium	+/1	+/2	+/5	+/4	+/4	+/7	+/1	-	-	-	-	+/1	+/1
Phocaeicola	+/4	+/4	+/4	+/3	+/5	+/4	+/5	+/5	+/6	+/4	+/6	+/6	+/1
Prevotella	-	+/1	-	-	+/1	-	-	+/2	+/2	+/1	+/2	+/1	-
Prevotellamassilia	-	+/1	-	-	+/1	-		-			-		-
Roseburia	-	+/1	+/2	-	+/1	+/1	+/1	-	-	+/2	+/1	+/2	-

Ruminococcus	+/4	+/3	+/2	+/5	+/1	+/1	+/1	+/2	+/4	+/3	+/2	+/3	+/1
Sutterella	-	+/1	+/3	+/2	+/4	+/2	+/2	+/1	-	+/1	+/1	-	-
Unclassified Clostridiales	-	+/1	+/2	+/1	+/1	+/3	+/3	+/4	+/4	+/3	+/2	+/2	-
Unclassified Erysipelotrichaceae	+/1	+/1	-		-		+/1	-	-	+/1	-	-	-
Unclassified Firmicutes	-	-	+/1	-	+/3	+/2	-	+/2	+/1	+3	+/1	-	-
Unclassified Lachnospiraceae	+/4	+/2	+/3	+/3	+/3	+/4	+/4	-	-	+/4	-	+/1	-
Unclassified Ruminococcaceae	+/1	+/2	+/1	+/1	+/3	+/4	+/2	+/5	+/6	+3	+/4	+/6	-

Chapter 4: Discussion

Every person has a unique gut microbiome, often called a "microbial fingerprint" [79]. Just as no two individuals have the same genetic code, the microbial communities inhabiting their gastrointestinal tracts are similarly diverse. This unique composition of microorganisms is shaped by a various of factors including genetics, diet, medications, lifestyle, and environmental influences [6], [7]. These microbial communities play an essential role in health, influencing processes such as digestion, metabolism, immune function, and even mental health [21], [19]. The diversity and specificity of each individual's microbiome means that responses to dietary interventions, prebiotics, and other factors can vary significantly, making personalized approaches essential for understanding and optimizing gut health [80]. This variation in responses underscores the importance of identifying compounds, like prebiotics, that have the potential to universally benefit gut health, while still accounting for individual differences in microbiome composition. Prebiotics have been extensively studied for their beneficial properties across a broad spectrum of individuals, despite variations in their microbiota.

Prebiotics are compounds that utilized by specific microorganisms of the host and provide health benefits [40]. They promote the growth of probiotics like *Bifidobacterium* and *Lactobacillus*, which are integral to maintaining gut health as they are engaged in production of short-chain fatty acids (SCFAs), affect the immune system, and enhancement of gut barrier integrity [41], [43]. Among various prebiotics, arabinogalactan stands out for its unique composition of complex polysaccharides derived from plant cell walls [49]. As a non-digestible carbohydrate, arabinogalactan exhibited a more persistent fermentation profile in the distal colon compared to fructo-oligosaccharides (FOS) [81]. AG demonstrated to help maintain metabolic homeostasis and the prevention of metabolic diseases including obesity and improving insulin level by influencing the tryptophan and galactose pathways and facilitating the digestion and absorption of carbohydrates [82], [83]. It undergoes fermentation by gut microbes and accelerates the proliferation of beneficial bacteria

including *Bifidobacterium*, *Faecalibacterium, Bacteroidetes* and *Lactobacillus* [81], [84], [85]. Furthermore, AG degradation by gut microbiota leads to the production of SCFAs like propionate and butyrate in regions of the colon where substrate availability is typically lower, while inhibiting the accumulation of potentially harmful compounds like sulfide and indole [86], [51]. This selective stimulation of beneficial microbes highlights arabinogalactan's role in shaping microbial communities and promoting gut health such as affecting the mucus layer, making it an ideal candidate for exploring personalized microbiome interventions [87].

Despite these potential universal benefits of arabinogalactan, the specific microbial responses to prebiotic treatments can vary significantly between people. A study showed that individual microbiome composition played a stronger role in determining prebiotic responses than the specific type of prebiotic used [88]. For example, differences in short-chain fatty acid production in response to various prebiotics, including wheat dextrin, galactooligosaccharides, and inulin suggested that individual microbiomes had a unique capacity to metabolize these compounds. This heterogeneity was further impacted by baseline fiber intake, as those who consumed more fiber on a regular basis showed less of a shift in SCFA production after taking prebiotic supplements. These findings suggest that personalized microbiota therapies may be more effective than a "one size fits all" treatment [88]. A recent review highlighted how both ecological factors (like niche availability) and molecular factors (such as the presence of prebiotic-utilization genes) play critical roles in whether an individual will respond to prebiotic treatments. This explains why certain individuals, despite receiving the same prebiotic, may have vastly different microbial responses due to differences in their baseline microbiota composition and genetic capabilities [89] . In particular, a study showed that the utilization of Gum Arabic AG protein by *Bifidobacterium longum* subsp. *Longum* was strain-dependent, with only certain strains possessed the genes necessary to efficiently metabolize arabinogalactan, which further explained the variability in microbial responses [90].

The unique fingerprint of bacterial communities was evident also throughout all stages of this study. PCA analysis highlighted a significant inter-individual effect ($p=0.001$), surpassing the impact of treatment and incubation time (Figure 3 & 4). Such variations likely stem from

intrinsic factors unique to each donor, which may not be directly influenced by short-term dietary interventions but significantly impact the baseline and responsive behavior of the microbiome. Notably, donors 2 and 10 exhibited distinct clustering compared to other participants. Although specific details about donor 10 were limited, its distinct profile may be attributed to genetic, lifestyle, dietary factors, or a combination of these elements influencing microbiota composition. Furthermore, consistent with findings from other studies, the gut microbiome of vegetarians often differs from that of non-vegetarians, typically showing higher levels of bacteria like *Prevotella*, which is associated with fiber breakdown [91]. This study confirmed that *Prevotella* was the most abundant genus in donor 2 compared to the other individuals. In addition, this donor demonstrated the only individual with enrichment in *Mitsuokella* at both time points incubation with AG in microcosm samples and the active fraction of 6h. While *Mitsuokella* has not been specifically reported to degrade arabinogalactan, *Mitsuokella jalaludinii* has demonstrated probiotic potential, inhibiting pathogenic bacteria and promoting gut health in animal models [92].

Considering these variations, similar trends were observed in individuals. For instance, arabinogalactan altered the relative abundance of bacterial populations at the phylum level in all donors, although the extent of these changes varied among individuals' fecal samples (Figure 5). The varied responses across phyla suggested differential metabolic capabilities or competitive advantages conferred by AG treatment. For example, the consistent increase in *Actinobacteria* across most donors likely indicates the enrichment of *Bifidobacterium* and *Collinsella* as arabinogalactan consumers, given their significant increases at the genus level ($p=0.04$ and $p=0.03$, respectively) in the microcosm samples (Figures 9 & 10). This pattern was further corroborated by RACS results, where the majority of the isolates were identified as *Bifidobacterium longum* and *Collinsella aerofaciens* (Figure 14).

Ability of *B. longum* for consuming AG is well documented [52], [93], [86]. Studies have shown that key enzymes involved in AG degradation include β-galactanases, β-galactosidases, α-L-arabinofuranosidases, and β-L-arabinopyranosidases and while *B. longum* could partially degrade AG in monoculture, its growth and AG degradation were enhanced in coculture with other bacteria like *Bacteroides caccae* [84], [94]. Furthermore,

a study reported a synergistic interaction between AG and a probiotic strain of *B. longum* that increased butyrate synthesis and enhanced the number of *Faecalibacterium prausnitzii* in the transverse colon [86]. Also, combination of AG with these two strains demonstrated probiotics in gut, such as *Lactococcus* and consequently, positive impacts on metabolic health by decreasing weight, reducing fat storage, and enhancing sensitivity to insulin in rodents [95]. In the current study *Lactococcus* were exclusively enriched in the presence of AG. Some species of this genus, particularly *Lactococcus lactis*, are considered potential probiotics due to their common use in fermented dairy products and their involvement to gut health. However, some concerns about their pathogenicity have been raised [96].

B. longum is a well-studied probiotic bacterium that offers numerous health benefits. It enhances immune function by stimulating the immune system and has anti-inflammatory effects, primarily through the production of SCFAs like acetate [97]. This bacterium also plays a important role in metabolizing complex carbohydrates and fibers, supporting overall gut health that strengthens the gut barrier, protecting against harmful pathogens [98] ,[35]. Moreover, *B. longum* has been linked to beneficial effects on mental well-being via promoting the gut-brain axis, which could mitigate depression and anxiety through the modulation of gut bacteria and inflammation [99].

Based on literature there is no report of AG utilization by *C. aerofaciens*, however it can degrader other polysaccharides like inulin and arabinoxylans [42], [100].It is associated with improved clinical outcomes in non-constipated IBS (Irritable bowel syndrome) patients, where its abundance correlates with positive responses to probiotic treatments and has been identified as a potential marker for predicting the efficacy of probiotics, suggesting its role in enhancing gut microbiome balance [101]. This bacterium is capable of producing butyric acid which can alleviate various inflammatory diseases [102]. Also, it may potentially benefit health by influencing bile acids, which could modulate pathogen virulence and host cholesterol levels [103].

However, unlike the microcosm samples, the analysis of the active fraction did not clearly show the enrichment of *Bifidobacterium* and *Collinsella* in Ag treatment among the donors.

Additionally, lower abundances were observed across most genera at 24 hours. One possible explanation was that excessive bacterial growth may have interfered with the sorting process during FACS. High cell density can lead to aggregation, causing signal overlap or clogging the instrument, potentially resulting in false negatives and excluding larger aggregates from analysis [104]. Another possibility could be the attachment of bacteria to Ag molecules that was not recognized by the FCAS as a single cell. This was particularly relevant given the observed enrichment of *Bifidobacterium* in arabinose and galactose treatments. However, further investigation is required to identify the primary issue and potential contributing factors

The study also confirmed significant growth of *Bacteroides* and *Faecalibacterium* in the presence of AG, both known for their ability to degrade arabinogalactan. These genera were also recovered from RACS, showing the presence of *Bacteroides stercoris*, *Bacteroides uniformis*, and *F. prausnitzii*. Similarly, a study evaluated the fermentation of arabinogalactan extracted from *Lycium barbarum* (LBP-3) by *Bacteroides* species, such as *Bacteroides caccae* and *Phocaeicola vulgatus* and demonstrated their role in AG degradation and the production of beneficial fermentation products like oligosaccharides. This fermentation process also influenced the growth of other microbial species like *Parabacteroides*, illustrating the cooperative interactions within the gut microbiome [105]. Enrichment of *Phocaeicola* genus and isolation of *P. coprocola* was also obtained from the study. These findings along with other studies supported the potential of *Bacteroides* species as next-generation probiotics (NGP) because of their role in regulation of lymphocytes, cytokine expression, anti-inflammatory effects and their ability to modulate metabolism through the breakdown of complex carbohydrates like arabinogalactan [106].

For instance, *B. stercoris* abundance correlated positively with adherence to healthy diets, such as increased fiber, grain products, and vegetable intake, and has shown positive impacts against obesity in both in vitro and in vivo studies [107], [108]. Moreover, *F. prausnitzii* is emerging as a significant probiotic with multiple health benefits, particularly in promoting gut health, enhancing immune responses, and regulating metabolism [109]. Research indicated that *F. prausnitzii* supplementation can improve intestinal barrier

function, reduce inflammation, and restore gut microbiota balance, particularly after disruptions such as sleep deprivation [110]. Furthermore, its potential antiatherosclerotic properties highlight its importance in cardiovascular health, as it may aid in reducing the risk of inflammation and coronary artery disease [111]. As a SCFA producing probiotic, *F. prausnitzii* has also been associated with cognitive function and emotional well-being, showing potential as a psychobiotic [112]. Also, *Parabacteroides* species have been suggested to exhibit positive effects, with studies indicating their potential for development as probiotics for treating specific conditions [113]. For example, *P. merdae* has been shown to protect against obesity-associated atherosclerosis in an animal study [114].

Phascolarctobacterium and Blautia, two genera of bacteria found in the human gut microbiome, demonstrated increase in abundance when arabinogalactan is present in the diet [51]. This finding was consistent with the results of the current study under discussion. Although *Phascolarctobacterium* and *Blautia* are not typically included in common probiotic formulations, they play important roles in gut health and have shown probiotic potential. Particularly *Blautia* that is associated with the degradation of complex carbohydrates and has been linked to improved metabolic health. Some studies have suggested that higher levels of *Blautia* may be correlated with lower risks of obesity and type 2 diabetes [115]. *Phascolarctobacterium* is also known for its ability to produce SCFAs, particularly propionate and may help regulate appetite and glucose metabolism [116].

Significant growth of *Akkermansia* from *Verrucomicrobia* phylum was observed in some donors across both sample types (microcosm and BONCAT positive). Other studies have also reported that AG can positively influence the abundance of this genus, particularly *A. muciniphila* [117], [86]. This species is known for its ability to degrade mucin and protect the gut from pathogen colonization [118]. Additionally, research has shown that AG stimulates the production of specific glycans in the gut, which in turn promotes the enrichment of *A. muciniphila* [87]. The European Food Safety Authority (EFSA) has approved the pasteurized form of *A. muciniphila* [119]. As, a next generation probiotic, this species has shown promising effects in managing metabolic disorders such as obesity and diabetes [120], [121]. Its benefits, however, extend beyond metabolic related diseases, with emerging

research indicating its potential in improving brain health and addressing neurological disorders [122].

There is limited information available regarding the ability of the other identified strains to degrade arabinogalactan, but several of them are known to possess beneficial properties on health or probiotic potential. For example, *Alistipes* genus has garnered attention for its complex role in human health, with both protective and pathogenic effects, as evidenced by their links to mental health issues, cancer, and inflammation [123].

In addition, *Ruminococcus bicirculans* may play a protective role against the development of cardiopulmonary diseases. A decrease in this species has been associated with more severe pulmonary arterial hypertension (PAH), suggesting its potential role in cardiopulmonary health[124]. The *Lachnospiraceae* family, which includes several strains isolated in this study, is well-known for producing SCFAs, particularly butyrate that support gut barrier integrity. These bacteria are also specialists in degrading complex plant materials, further highlighting their importance in maintaining a healthy gut microbiome [125]. Moreover, reduced abundance of *Agathobacter*, a member of the *Lachnospiraceae* family, has been associated with sleep troubles and core signs in children with autism spectrum disorder (ASD), underscoring the importance of this genus in neurological health [126]. Additionally, the significant growth of *Gemmiger* in AG treatment in microcosm samples suggested its involvement in health, as previous studies have linked lower abundance of this genus to type 2 diabetes and IBS [127], [128] .

Fusicatenibacter, another genus showing growth in AG treatment, may have anti-inflammatory properties and has been suggested as a potential biomarker for distinguishing rheumatoid arthritis from healthy controls [129]. On the other hand, research on *Faecalibacillus* is still limited due to its recent discovery, but it demonstrated notable increases in some donors amended with AG, hinting at its potential health benefits that warrant further investigation.

The overall comparison of all donors in the 24h microcosm samples revealed significant changes in two butyrate producing bacteria: *Anaerobutyricum* and *Anaerostipes* (Figure 6).

However, these changes were not evident for each donor, likely due to their low abundance. Despite this, species of *Anaerobutyricum*, especially *A. soehngenii* and *A. hallii* have been proposed as NGP [130], [131]. The promising species include *Anaerobutyricum soehngenii* and *Anaerobutyricum hallii* have been shown potential benefits for metabolic health such as insulin sensitivity, type 2 diabetes and glucose metabolism [132], [133]. In addition, research has shown that *Anaerostipes* can be enriched by certain prebiotics, including inulin, FOSs and lactulose [42], [134], [135]. Although *Anaerostipes* is not yet classified as a probiotic, its ability to produce SCFAs, combined with its increased abundance in response to prebiotics, suggests that it holds potential for further investigation as a candidate for probiotic development.

RACS results indicated that *Dysosmobacter welbionis* was an active bacterium in the presence of AG. This newly discovered butyrate-producing bacterium from the human gut has demonstrated several positive health properties [136], [137]. Notably, the *D. welbionis* J115 strain has shown promising effects in controlling weight gain, improving lipid metabolism, and reducing inflammation that make it a new candidate as NGP [137], [138]. *Catenibacterium mitsuokai* also was another bacterium that recovered from this experiment. Previous studies have observed the enrichment of this genus in the presence of inulin that suggested a possible link between the bacterium and metabolic health issues related to diet [139], [140]. Additionally, an animal study demonstrated a significant correlation between *Catenibacterium* and elevated levels of SCFAs such as lactate, formate, and acetate, indicating its potential role in health benefits. However, further researches are necessary to fully understand its impacts [141].

The findings of this study underscored the complexity and individuality of the gut microbiome and its response to dietary interventions, such as arabinogalactan supplementation. While certain genera consistently showed enrichment across donors, the varying responses observed in other bacteria highlighted the significant role of individual microbiota composition. This variability emphasized the need for personalized approaches

in microbiome research and treatment. Customizing interventions based on a person's unique microbiome composition could enhance the efficacy of treatments, whether through prebiotics, probiotics, or other microbiota-targeted therapies. Personalized strategies not only account for individual variability but also maximize the potential for positive health outcomes, particularly in managing metabolic disorders, gastrointestinal health, and beyond.

Overall, the methodologies used in this study revealed a diverse range of AG-degrading genera, even though the results did not always coincide due to variances in activity markers and methodological differences. However, they highlighted the greater efficiency of these methods compared to traditional cultivation-based techniques. As previously discussed, some of the identified bacteria have not been reported to metabolize arabinogalactan, warranting further investigation to confirm their potential. However, the potential health benefits of arabinogalactan were demonstrated by its ability to promote the growth of beneficial microbial populations. This aligned with the growing understanding that prebiotics can selectively enhance beneficial species, even if the exact influences are not yet completely discovered. To this end, more studies are required, including monitoring mono- and co-cultures of the identified strains, assessing their AG degradation rates and enzyme activities, tracking short-chain fatty acid production, and conducting clinical trials to evaluate their prebiotic effectiveness in various diseases. Such research would help to elucidate the mechanisms behind arabinogalactan's effects on different microbial species and explore its broader implications for gut health, including its potential use in developing next-generation probiotics.

References

[1] S. Leviatan, S. Shoer, D. Rothschild, M. Gorodetski, and E. Segal, 'An expanded reference map of the human gut microbiome reveals hundreds of previously unknown species', *Nat. Commun.*, vol. 13, no. 1, p. 3863, 2022.

[2] K. Hou *et al.*, 'Microbiota in health and diseases', *Signal Transduct. Target. Ther.*, vol. 7, no. 1, p. 135, Apr. 2022, doi: 10.1038/s41392-022-00974-4.

[3] M. M. Rahman *et al.*, 'The gut microbiota (microbiome) in cardiovascular disease and its therapeutic regulation', *Front. Cell. Infect. Microbiol.*, vol. 12, p. 903570, 2022.

[4] J. C. Madan *et al.*, 'Association of cesarean delivery and formula supplementation with the intestinal microbiome of 6-week-old infants', *JAMA Pediatr.*, vol. 170, no. 3, pp. 212–219, 2016.

[5] F. Yasmin *et al.*, 'Cesarean section, formula feeding, and infant antibiotic exposure: separate and combined impacts on gut microbial changes in later infancy', *Front. Pediatr.*, vol. 5, p. 288753, 2017.

[6] J. Yang *et al.*, 'Gut bacteria formation and influencing factors', *FEMS Microbiol. Ecol.*, vol. 97, no. 4, p. fiab043, 2021.

[7] N. Hasan and H. Yang, 'Factors affecting the composition of the gut microbiota, and its modulation', *PeerJ*, vol. 7, p. e7502, 2019.

[8] E. Rinninella *et al.*, 'What is the healthy gut microbiota composition? A changing ecosystem across age, environment, diet, and diseases', *Microorganisms*, vol. 7, no. 1, p. 14, 2019.

[9] E. M. M. Quigley, 'Gut bacteria in health and disease.', *Gastroenterol. Hepatol.*, vol. 9, no. 9, pp. 560–569, Sep. 2013.

[10] P. B. Eckburg *et al.*, 'Diversity of the human intestinal microbial flora', *science*, vol. 308, no. 5728, pp. 1635–1638, 2005.

[11] A. Oren and G. M. Garrity, 'Valid publication of the names of forty-two phyla of prokaryotes', *Int. J. Syst. Evol. Microbiol.*, vol. 71, no. 10, p. 005056, 2021.

[12] S. Ahlawat, Asha, and K. K. Sharma, 'Gut–organ axis: a microbial outreach and networking', *Lett. Appl. Microbiol.*, vol. 72, no. 6, pp. 636–668, 2021.

[13] M. O. Welcome and M. O. Welcome, 'Functional relationship between the gut and other tissues/organs of the body', *Gastrointest. Physiol. Dev. Princ. Mech. Regul.*, pp. 1009–1028, 2018.

[14] P. Vernocchi, F. Del Chierico, and L. Putignani, 'Gut microbiota metabolism and interaction with food components', *Int. J. Mol. Sci.*, vol. 21, no. 10, p. 3688, 2020.

[15] E. Capuano, 'The behavior of dietary fiber in the gastrointestinal tract determines its physiological effect', *Crit. Rev. Food Sci. Nutr.*, vol. 57, no. 16, pp. 3543–3564, 2017.

[16] S. Sanna *et al.*, 'Causal relationships among the gut microbiome, short-chain fatty acids and metabolic diseases', *Nat. Genet.*, vol. 51, no. 4, pp. 600–605, 2019.

[17] D. J. Morrison and T. Preston, 'Formation of short chain fatty acids by the gut microbiota and their impact on human metabolism', *Gut Microbes*, vol. 7, no. 3, pp. 189–200, 2016.

[18] V. T. Pham, S. Dold, A. Rehman, J. K. Bird, and R. E. Steinert, 'Vitamins, the gut microbiome and gastrointestinal health in humans', *Nutr. Res.*, vol. 95, pp. 35–53, 2021.

[19] S. M. O'Mahony, G. Clarke, Y. E. Borre, T. G. Dinan, and J. F. Cryan, 'Serotonin, tryptophan metabolism and the brain-gut-microbiome axis', *Behav. Brain Res.*, vol. 277, pp. 32–48, 2015.

[20] W. M. De Vos, H. Tilg, M. Van Hul, and P. D. Cani, 'Gut microbiome and health: mechanistic insights', *Gut*, vol. 71, no. 5, pp. 1020–1032, 2022.

[21] E. Z. Gomaa, 'Human gut microbiota/microbiome in health and diseases: a review', *Antonie Van Leeuwenhoek*, vol. 113, no. 12, pp. 2019–2040, 2020.

[22] T. Takiishi, C. I. M. Fenero, and N. O. S. Câmara, 'Intestinal barrier and gut microbiota: Shaping our immune responses throughout life', *Tissue Barriers*, vol. 5, no. 4, p. e1373208, 2017.

[23] B. Bonaz, T. Bazin, and S. Pellissier, 'The vagus nerve at the interface of the microbiota-gut-brain axis', *Front. Neurosci.*, vol. 12, p. 336468, 2018.

[24] P. Strandwitz *et al.*, 'GABA-modulating bacteria of the human gut microbiota', *Nat. Microbiol.*, vol. 4, no. 3, pp. 396–403, 2019.

[25] A. N. Varanoske *et al.*, 'Stress and the gut-brain axis: Cognitive performance, mood state, and biomarkers of blood-brain barrier and intestinal permeability following severe physical and psychological stress', *Brain. Behav. Immun.*, vol. 101, pp. 383–393, 2022.

[26] S. Carding, K. Verbeke, D. T. Vipond, B. M. Corfe, and L. J. Owen, 'Dysbiosis of the gut microbiota in disease', *Microb. Ecol. Health Dis.*, vol. 26, no. 0, Feb. 2015, doi: 10.3402/mehd.v26.26191.

[27] I. N. Grigor'eva, 'Gallstone disease, obesity and the firmicutes/bacteroidetes ratio as a possible biomarker of gut dysbiosis', *J. Pers. Med.*, vol. 11, no. 1, p. 13, 2020.

[28] M. T. Alam, G. C. Amos, A. R. Murphy, S. Murch, E. M. Wellington, and R. P. Arasaradnam, 'Microbial imbalance in inflammatory bowel disease patients at different taxonomic levels', *Gut Pathog.*, vol. 12, pp. 1–8, 2020.

[29] P. T. Santana, S. L. B. Rosas, B. E. Ribeiro, Y. Marinho, and H. S. de Souza, 'Dysbiosis in inflammatory bowel disease: pathogenic role and potential therapeutic targets', *Int. J. Mol. Sci.*, vol. 23, no. 7, p. 3464, 2022.

[30] H. C. Mirsepasi-Lauridsen, B. A. Vallance, K. A. Krogfelt, and A. M. Petersen, 'Escherichia coli pathobionts associated with inflammatory bowel disease', *Clin. Microbiol. Rev.*, vol. 32, no. 2, p. 10.1128/cmr. 00060-18, 2019.

[31] S. Sonali *et al.*, 'Mechanistic insights into the link between gut dysbiosis and major depression: an extensive review', *Cells*, vol. 11, no. 8, p. 1362, 2022.

[32] U. Shabbir, M. S. Arshad, A. Sameen, and D.-H. Oh, 'Crosstalk between gut and brain in Alzheimer's disease: the role of gut microbiota modulation strategies', *Nutrients*, vol. 13, no. 2, p. 690, 2021.

[33] R.-G. Xiong *et al.*, 'The role of gut microbiota in anxiety, depression, and other mental disorders as well as the protective effects of dietary components', *Nutrients*, vol. 15, no. 14, p. 3258, 2023.

[34] F. A. O. Joint, 'Health and Nutritional Properties of Probiotics in Food including Powder Milk with Live Lave Lactic Acid Bacteria. Ref Tye Report', *Httpwww Who Intfoodsagetypublicationsfsmanagementenprobiotics Pdf*, 2001, Accessed: Jun. 14, 2024. [Online]. Available: https://cir.nii.ac.jp/crid/1572261549180955904

[35] E. Stavropoulou and E. Bezirtzoglou, 'Probiotics in medicine: a long debate', *Front. Immunol.*, vol. 11, p. 2192, 2020.

[36] Q. CEN, R. PANG, Y. CUI, J. WEI, and A. ZHANG, 'Advances in the Mechanism of Lactobacillus rhamnosus GG Improving Inflammatory Bowel Disease', *Chin. Gen. Pract.*, vol. 25, no. 36, p. 4595, 2022.

[37] Z. F. Ma *et al.*, 'Bifidobacterium infantis M-63 improves mental health in victims with irritable bowel syndrome developed after a major flood disaster', *Benef. Microbes*, vol. 10, no. 2, pp. 111–120, 2019.

[38] P. Pais, V. Almeida, M. Yılmaz, and M. C. Teixeira, 'Saccharomyces boulardii: what makes it tick as successful probiotic?', *J. Fungi*, vol. 6, no. 2, p. 78, 2020.

[39] P. Kesika, N. Suganthy, B. S. Sivamaruthi, and C. Chaiyasut, 'Role of gut-brain axis, gut microbial composition, and probiotic intervention in Alzheimer's disease', *Life Sci.*, vol. 264, p. 118627, 2021.

[40] G. R. Gibson and M. B. Roberfroid, 'Dietary modulation of the human colonic microbiota: introducing the concept of prebiotics', *J. Nutr.*, vol. 125, no. 6, pp. 1401–1412, 1995.

[41] E. M. Quigley, 'Prebiotics and probiotics; modifying and mining the microbiota', *Pharmacol. Res.*, vol. 61, no. 3, pp. 213–218, 2010.

[42] A. Riva *et al.*, 'Identification of inulin-responsive bacteria in the gut microbiota via multi-modal activity-based sorting', *Nat. Commun.*, vol. 14, no. 1, p. 8210, 2023.

[43] S. You *et al.*, 'The promotion mechanism of prebiotics for probiotics: A review', *Front. Nutr.*, vol. 9, p. 1000517, 2022.

[44] A. K. Samanta *et al.*, 'Xylooligosaccharides as prebiotics from agricultural by-products: Production and applications', *Bioact. Carbohydr. Diet. Fibre*, vol. 5, no. 1, pp. 62–71, 2015.

[45] C. Nobre, L. S. Simões, D. A. Gonçalves, P. Berni, and J. A. Teixeira, 'Fructooligosaccharides production and the health benefits of prebiotics', in *Current developments in biotechnology and*

bioengineering, Elsevier, 2022, pp. 109–138. Accessed: Jun. 14, 2024. [Online]. Available: https://www.sciencedirect.com/science/article/pii/B9780128235065000023

[46] D. P. M. Torres, M. D. P. F. Gonçalves, J. A. Teixeira, and L. R. Rodrigues, 'Galacto-Oligosaccharides: Production, Properties, Applications, and Significance as Prebiotics', *Compr. Rev. Food Sci. Food Saf.*, vol. 9, no. 5, pp. 438–454, Sep. 2010, doi: 10.1111/j.1541-4337.2010.00119.x.

[47] A. Nath *et al.*, 'Biochemical activities of lactose-derived prebiotics—A review', *Acta Aliment.*, vol. 46, no. 4, pp. 449–456, 2017.

[48] B. Wilson and K. Whelan, 'Prebiotic inulin-type fructans and galacto-oligosaccharides: definition, specificity, function, and application in gastrointestinal disorders', *J. Gastroenterol. Hepatol.*, vol. 32, pp. 64–68, 2017.

[49] G. S. Kelly, 'Larch arabinogalactan: clinical relevance of a novel immune-enhancing polysaccharide.', *Altern. Med. Rev. J. Clin. Ther.*, vol. 4, no. 2, pp. 96–103, 1999.

[50] G. T. Macfarlane, H. Steed, and S. Macfarlane, 'Bacterial metabolism and health-related effects of galacto-oligosaccharides and other prebiotics', *J. Appl. Microbiol.*, vol. 104, no. 2, pp. 305–344, 2008.

[51] Y. Sun *et al.*, 'Prebiotic characteristics of arabinogalactans during in vitro fermentation through multi-omics analysis', *Food Chem. Toxicol.*, vol. 156, p. 112522, 2021.

[52] K. Fujita, Y. Sasaki, and K. Kitahara, 'Degradation of plant arabinogalactan proteins by intestinal bacteria: characteristics and functions of the enzymes involved', *Appl. Microbiol. Biotechnol.*, vol. 103, no. 18, pp. 7451–7457, Sep. 2019, doi: 10.1007/s00253-019-10049-0.

[53] C. Dion, E. Chappuis, and C. Ripoll, 'Does larch arabinogalactan enhance immune function? A review of mechanistic and clinical trials', *Nutr. Metab.*, vol. 13, no. 1, p. 28, Dec. 2016, doi: 10.1186/s12986-016-0086-x.

[54] T. Velikova *et al.*, 'Lactobacilli supplemented with larch arabinogalactan and colostrum stimulates an immune response towards peripheral NK activation and gut tolerance', *Nutrients*, vol. 12, no. 6, p. 1706, 2020.

[55] W. Huang *et al.*, 'A new perspective on structural characterisation and immunomodulatory activity of arabinogalactan in Larix kaempferi from Qinling Mountains', *Int. J. Biol. Macromol.*, vol. 265, p. 130859, 2024.

[56] J.-C. Lagier, S. Edouard, I. Pagnier, O. Mediannikov, M. Drancourt, and D. Raoult, 'Current and past strategies for bacterial culture in clinical microbiology', *Clin. Microbiol. Rev.*, vol. 28, no. 1, pp. 208–236, 2015.

[57] M. Bonnet, J. C. Lagier, D. Raoult, and S. Khelaifia, 'Bacterial culture through selective and non-selective conditions: the evolution of culture media in clinical microbiology', *New Microbes New Infect.*, vol. 34, p. 100622, 2020.

[58] M. H. Fraher, P. W. O'toole, and E. M. Quigley, 'Techniques used to characterize the gut microbiota: a guide for the clinician', *Nat. Rev. Gastroenterol. Hepatol.*, vol. 9, no. 6, pp. 312–322, 2012.

[59] D. Tegtmeier, S. Hurka, S. Mihajlovic, M. Bodenschatz, S. Schlimbach, and A. Vilcinskas, 'Culture-independent and culture-dependent characterization of the black soldier fly gut microbiome reveals a large proportion of culturable bacteria with potential for industrial applications', *Microorganisms*, vol. 9, no. 8, p. 1642, 2021.

[60] R. Hatzenpichler, S. Scheller, P. L. Tavormina, B. M. Babin, D. A. Tirrell, and V. J. Orphan, 'In situ visualization of newly synthesized proteins in environmental microbes using amino acid tagging and click chemistry', *Environ. Microbiol.*, vol. 16, no. 8, pp. 2568–2590, 2014.

[61] M. Taguer, B. J. Shapiro, and C. F. Maurice, 'Translational activity is uncoupled from nucleic acid content in bacterial cells of the human gut microbiota', *Gut Microbes*, vol. 13, no. 1, p. 1903289, 2021.

[62] A. Leizeaga, M. Estrany, I. Forn, and M. Sebastián, 'Using click-chemistry for visualizing in situ changes of translational activity in planktonic marine bacteria', *Front. Microbiol.*, vol. 8, p. 2360, 2017.

[63] T. D. Valentini *et al.*, 'Bioorthogonal non-canonical amino acid tagging reveals translationally active subpopulations of the cystic fibrosis lung microbiota', *Nat. Commun.*, vol. 11, no. 1, p. 2287, 2020.

[64] M. Wagner, 'Single-cell ecophysiology of microbes as revealed by Raman microspectroscopy or secondary ion mass spectrometry imaging', *Annu. Rev. Microbiol.*, vol. 63, no. 1, pp. 411–429, 2009.

[65] K. Klein *et al.*, 'Label-free live-cell imaging with confocal Raman microscopy', *Biophys. J.*, vol. 102, no. 2, pp. 360–368, 2012.

[66] G. Pezzotti, 'Raman spectroscopy in cell biology and microbiology', *J. Raman Spectrosc.*, vol. 52, no. 12, pp. 2348–2443, 2021.

[67] W. E. Huang *et al.*, 'Raman-FISH: combining stable-isotope Raman spectroscopy and fluorescence in situ hybridization for the single cell analysis of identity and function', *Environ. Microbiol.*, vol. 9, no. 8, pp. 1878–1889, 2007.

[68] Y. Wang, W. E. Huang, L. Cui, and M. Wagner, 'Single cell stable isotope probing in microbiology using Raman microspectroscopy', *Curr. Opin. Biotechnol.*, vol. 41, pp. 34–42, 2016.

[69] K. S. Lee *et al.*, 'Optofluidic Raman-activated cell sorting for targeted genome retrieval or cultivation of microbial cells with specific functions', *Nat. Protoc.*, vol. 16, no. 2, pp. 634–676, 2021.

[70] X. Wang, N. Liu, Y. Zhao, F. Yang, Z. Zhu, and D. Song, 'Research progress in the medical application of heavy water, especially in the field of D2O-Raman spectroscopy', *Int. J. Med. Sci.*, vol. 19, no. 8, p. 1357, 2022.

[71] D. Berry *et al.*, 'Tracking heavy water (D2O) incorporation for identifying and sorting active microbial cells', *Proc. Natl. Acad. Sci.*, vol. 112, no. 2, pp. E194–E203, 2015.

[72] A. L. Sessions, L. L. Jahnke, A. Schimmelmann, and J. M. Hayes, 'Hydrogen isotope fractionation in lipids of the methane-oxidizing bacterium Methylococcus capsulatus', *Geochim. Cosmochim. Acta*, vol. 66, no. 22, pp. 3955–3969, 2002.

[73] K. Hodne and F.-A. Weltzien, 'Single-cell isolation and gene analysis: pitfalls and possibilities', *Int. J. Mol. Sci.*, vol. 16, no. 11, pp. 26832–26849, 2015.

[74] K. S. Lee *et al.*, 'An automated Raman-based platform for the sorting of live cells by functional properties', *Nat. Microbiol.*, vol. 4, no. 6, pp. 1035–1048, 2019.

[75] K. Tamura, G. Stecher, and S. Kumar, 'MEGA11: molecular evolutionary genetics analysis version 11', *Mol. Biol. Evol.*, vol. 38, no. 7, pp. 3022–3027, 2021.

[76] D. T. Hoang, O. Chernomor, A. Von Haeseler, B. Q. Minh, and L. S. Vinh, 'UFBoot2: improving the ultrafast bootstrap approximation', *Mol. Biol. Evol.*, vol. 35, no. 2, pp. 518–522, 2018.

[77] A. von Haeseler, H. A. Schmidt, M. Q. Bui, and L. T. Nguyen, 'IQ-TREE: A fast and effective stochastic algorithm for estimating maximum-likelihood phylogenies', 2014.

[78] I. Letunic and P. Bork, 'Interactive Tree of Life (iTOL) v6: recent updates to the phylogenetic tree display and annotation tool', *Nucleic Acids Res.*, p. gkae268, 2024.

[79] L. Chen *et al.*, 'The long-term genetic stability and individual specificity of the human gut microbiome', *Cell*, vol. 184, no. 9, pp. 2302-2315. e12, 2021.

[80] E.-J. Song and J.-H. Shin, 'Personalized diets based on the gut microbiome as a target for health maintenance: from current evidence to future possibilities', *J. Microbiol. Biotechnol.*, vol. 32, no. 12, p. 1497, 2022.

[81] K. Terpend, S. Possemiers, D. Daguet, and M. Marzorati, 'Arabinogalactan and fructo-oligosaccharides have a different fermentation profile in the S imulator of the H uman I ntestinal M icrobial E cosystem (SHIME®)', *Environ. Microbiol. Rep.*, vol. 5, no. 4, pp. 595–603, 2013.

[82] J.-J. Wen *et al.*, 'Different dietary fibers unequally remodel gut microbiota and charge up anti-obesity effects', *Food Hydrocoll.*, vol. 140, p. 108617, 2023.

[83] Q. Nie *et al.*, 'Targeted modification of gut microbiota and related metabolites via dietary fiber', *Carbohydr. Polym.*, vol. 316, p. 120986, 2023.

[84] Y. Wang and G. LaPointe, 'Arabinogalactan utilization by Bifidobacterium longum subsp. longum NCC 2705 and Bacteroides caccae ATCC 43185 in monoculture and coculture', *Microorganisms*, vol. 8, no. 11, p. 1703, 2020.

[85] R. R. Robinson, J. Feirtag, and J. L. Slavin, 'Effects of dietary arabinogalactan on gastrointestinal and blood parameters in healthy human subjects', *J. Am. Coll. Nutr.*, vol. 20, no. 4, pp. 279–285, 2001.

[86] Y. Wang, Y. Liu, I. I. Polic, A. C. Matheyambath, and G. LaPointe, 'Modulation of human gut microbiota composition and metabolites by arabinogalactan and Bifidobacterium longum subsp. longum BB536 in the Simulator of the Human Intestinal Microbial Ecosystem (SHIME®)', *J. Funct. Foods*, vol. 87, p. 104820, 2021.

[87] T. Zhao *et al.*, 'Impact of structurally diverse polysaccharides on colonic mucin O-glycosylation and gut microbiota', *Npj Biofilms Microbiomes*, vol. 9, no. 1, p. 97, 2023.

[88] Z. C. Holmes *et al.*, 'Microbiota responses to different prebiotics are conserved within individuals and associated with habitual fiber intake', *Microbiome*, vol. 10, no. 1, p. 114, 2022.

[89] M. N. Ojima, K. Yoshida, M. Sakanaka, L. Jiang, T. Odamaki, and T. Katayama, 'Ecological and molecular perspectives on responders and non-responders to probiotics and prebiotics', *Curr. Opin. Biotechnol.*, vol. 73, pp. 108–120, 2022.

[90] Y. Sasaki *et al.*, 'Novel 3-O-α-D-galactosyl-α-L-arabinofuranosidase for the assimilation of gum arabic arabinogalactan protein in Bifidobacterium longum subsp. longum', *Appl. Environ. Microbiol.*, vol. 87, no. 10, pp. e02690-20, 2021.

[91] G. D. Wu *et al.*, 'Linking long-term dietary patterns with gut microbial enterotypes', *Science*, vol. 334, no. 6052, pp. 105–108, 2011.

[92] U. Y. Levine, S. M. Bearson, and T. B. Stanton, 'Mitsuokella jalaludinii inhibits growth of Salmonella enterica serovar Typhimurium', *Vet. Microbiol.*, vol. 159, no. 1–2, pp. 115–122, 2012.

[93] O. Chen, S. Sudakaran, T. Blonquist, E. Mah, S. Durkee, and A. Bellamine, 'Effect of arabinogalactan on the gut microbiome: A randomized, double-blind, placebo-controlled, crossover trial in healthy adults', *Nutrition*, vol. 90, p. 111273, 2021.

[94] K. Fujita, A. Sakamoto, S. Kaneko, T. Kotake, Y. Tsumuraya, and K. Kitahara, 'Degradative enzymes for type II arabinogalactan side chains in Bifidobacterium longum subsp. longum', *Appl. Microbiol. Biotechnol.*, vol. 103, pp. 1299–1310, 2019.

[95] H. He *et al.*, 'Arabinogalactan, Bifidobacterium longum, and Faecalibacterium prausnitzii improve insulin resistance in high-fat diet-induced C57BL/6J mice', *eFood*, vol. 3, no. 1–2, p. e1, 2022.

[96] F. Wu, X. Xie, T. Du, X. Jiang, W. Miao, and T. Wang, 'Lactococcus lactis, a bacterium with probiotic functions and pathogenicity', *World J. Microbiol. Biotechnol.*, vol. 39, no. 12, p. 325, 2023.

[97] S. Yao, Z. Zhao, W. Wang, and X. Liu, 'Bifidobacterium longum: protection against inflammatory bowel disease', *J. Immunol. Res.*, vol. 2021, no. 1, p. 8030297, 2021.

[98] S. Arboleya *et al.*, 'Gene-trait matching across the Bifidobacterium longum pan-genome reveals considerable diversity in carbohydrate catabolism among human infant strains', *BMC Genomics*, vol. 19, pp. 1–16, 2018.

[99] C. AnaMaria and D. C. Vodnar, 'Exploring the gut-brain Axis: Potential therapeutic impact of Psychobiotics on mental health', *Prog. Neuropsychopharmacol. Biol. Psychiatry*, p. 111073, 2024.

[100] I. Gu *et al.*, 'In vitro fecal fermentation patterns of arabinoxylan from rice bran on fecal microbiota from normal-weight and overweight/obese subjects', *Nutrients*, vol. 13, no. 6, p. 2052, 2021.

[101] G. Gargari *et al.*, 'Collinsella aerofaciens as a predictive marker of response to probiotic treatment in non-constipated irritable bowel syndrome', *Gut Microbes*, vol. 16, no. 1, p. 2298246, 2024.

[102] P. Qin, Y. Zou, Y. Dai, G. Luo, X. Zhang, and L. Xiao, 'Characterization a novel butyric acid-producing bacterium Collinsella aerofaciens subsp. shenzhenensis subsp. nov.', *Microorganisms*, vol. 7, no. 3, p. 78, 2019.

[103] S. Bag, T. S. Ghosh, and B. Das, 'Complete genome sequence of Collinsella aerofaciens isolated from the gut of a healthy Indian subject', *Genome Announc.*, vol. 5, no. 47, p. 10.1128/genomea. 01361-17, 2017.

[104] A. Cossarizza *et al.*, 'Guidelines for the use of flow cytometry and cell sorting in immunological studies', *Eur. J. Immunol.*, vol. 49, no. 10, pp. 1457–1973, 2019.

[105] C. Cao *et al.*, 'Interaction between Bacteroidetes species in the fermentation of Lycium barbarum arabinogalactan', *Food Chem.*, vol. 409, p. 135288, 2023.

[106] H. Tan, Q. Zhai, and W. Chen, 'Investigations of Bacteroides spp. towards next-generation probiotics', *Food Res. Int.*, vol. 116, pp. 637–644, 2019.

[107] L. Gaundal *et al.*, 'Gut microbiota is associated with dietary intake and metabolic markers in healthy individuals', *Food Nutr. Res.*, vol. 66, 2022.

[108] S. W. Ryu *et al.*, 'Anti-obesity activity of human gut microbiota Bacteroides stercoris KGMB02265', *Arch. Microbiol.*, vol. 206, no. 1, p. 19, 2024.

[109] X. He, S. Zhao, and Y. Li, 'Faecalibacterium prausnitzii: A Next-Generation Probiotic in Gut Disease Improvement', *Can. J. Infect. Dis. Med. Microbiol.*, vol. 2021, no. 1, p. 6666114, 2021.

[110] X. Wang *et al.*, 'Faecalibacterium prausnitzii Supplementation Prevents Intestinal Barrier Injury and Gut Microflora Dysbiosis Induced by Sleep Deprivation', *Nutrients*, vol. 16, no. 8, p. 1100, 2024.

[111] H.-T. Yang *et al.*, 'Faecalibacterium prausnitzii as a potential Antiatherosclerotic microbe', *Cell Commun. Signal.*, vol. 22, no. 1, p. 54, 2024.

[112] Z. Hao, W. Wang, R. Guo, and H. Liu, 'Faecalibacterium prausnitzii (ATCC 27766) has preventive and therapeutic effects on chronic unpredictable mild stress-induced depression-like and anxiety-like behavior in rats', *Psychoneuroendocrinology*, vol. 104, pp. 132–142, 2019.

[113] W. K. K. Wu, 'Parabacteroides distasonis: an emerging probiotic?', *Gut*, vol. 72, no. 9, pp. 1635–1636, 2023.

[114] S. Qiao *et al.*, 'Gut Parabacteroides merdae protects against cardiovascular damage by enhancing branched-chain amino acid catabolism', *Nat. Metab.*, vol. 4, no. 10, pp. 1271–1286, 2022.

[115] K. Hosomi *et al.*, 'Oral administration of Blautia wexlerae ameliorates obesity and type 2 diabetes via metabolic remodeling of the gut microbiota', *Nat. Commun.*, vol. 13, no. 1, p. 4477, 2022.

[116] Y. Xu, Y. Zhu, X. Li, and B. Sun, 'Dynamic balancing of intestinal short-chain fatty acids: The crucial role of bacterial metabolism', *Trends Food Sci. Technol.*, vol. 100, pp. 118–130, 2020.

[117] J. Chen *et al.*, 'Sarcodon aspratus polysaccharides ameliorated obesity-induced metabolic disorders and modulated gut microbiota dysbiosis in mice fed a high-fat diet', *Food Funct.*, vol. 11, no. 3, pp. 2588–2602, 2020.

[118] M. T. Sorbara and E. G. Pamer, 'Interbacterial mechanisms of colonization resistance and the strategies pathogens use to overcome them', *Mucosal Immunol.*, vol. 12, no. 1, pp. 1–9, 2019.

[119] N. F. and F. A. (NDA) EFSA Panel on Nutrition *et al.*, 'Safety of pasteurised Akkermansia muciniphila as a novel food pursuant to Regulation (EU) 2015/2283', *EFSA J.*, vol. 19, no. 9, p. e06780, 2021.

[120] C. Depommier *et al.*, 'Supplementation with Akkermansia muciniphila in overweight and obese human volunteers: a proof-of-concept exploratory study', *Nat. Med.*, vol. 25, no. 7, pp. 1096–1103, 2019.

[121] J. Li, G. Yang, Q. Zhang, Z. Liu, X. Jiang, and Y. Xin, 'Function of Akkermansia muciniphila in type 2 diabetes and related diseases', *Front. Microbiol.*, vol. 14, p. 1172400, 2023.

[122] R. Xu *et al.*, 'The role of the probiotic Akkermansia muciniphila in brain functions: insights underpinning therapeutic potential', *Crit. Rev. Microbiol.*, vol. 49, no. 2, pp. 151–176, 2023.

[123] B. J. Parker, P. A. Wearsch, A. C. Veloo, and A. Rodriguez-Palacios, 'The genus Alistipes: gut bacteria with emerging implications to inflammation, cancer, and mental health', *Front. Immunol.*, vol. 11, p. 906, 2020.

[124] A. Jose, S. Apewokin, W. E. Hussein, N. J. Ollberding, J. M. Elwing, and D. B. Haslam, 'A unique gut microbiota signature in pulmonary arterial hypertension: a pilot study', *Pulm. Circ.*, vol. 12, no. 1, p. e12051, 2022.

[125] A. Biddle, L. Stewart, J. Blanchard, and S. Leschine, 'Untangling the genetic basis of fibrolytic specialization by Lachnospiraceae and Ruminococcaceae in diverse gut communities', *Diversity*, vol. 5, no. 3, pp. 627–640, 2013.

[126] X. Hua *et al.*, 'The gut microbiota and associated metabolites are altered in sleep disorder of children with autism spectrum disorders', *Front. Psychiatry*, vol. 11, p. 855, 2020.

[127] W. Han, C. Huang, Y. Ji, L. Zhou, J. Chen, and J. Hou, 'Alterations in the gut microbiota and hepatitis-b-virus infection in Southern Chinese patients with coexisting non-alcoholic fatty liver disease and type-2 diabetes mellitus', *Front. Med.*, vol. 8, p. 805029, 2021.

[128] K. J. Kamp *et al.*, 'Bile acids and microbiome among individuals with irritable bowel syndrome and healthy volunteers', *Biol. Res. Nurs.*, vol. 23, no. 1, pp. 65–74, 2021.

[129] D. Yu *et al.*, *The gut microbiome and metabolites are altered and interrelated in patients with rheumatoid arthritis. Front Cell Infect Microbiol 11: 763507*. 2021.

[130] K. Wortelboer, A. M. Koopen, H. Herrema, W. M. de Vos, M. Nieuwdorp, and E. M. Kemper, 'From fecal microbiota transplantation toward next-generation beneficial microbes: The case of Anaerobutyricum soehngenii', *Front. Med.*, vol. 9, p. 1077275, 2022.

[131] M. Kumari *et al.*, 'Fostering next-generation probiotics in human gut by targeted dietary modulation: An emerging perspective', *Food Res. Int.*, vol. 150, p. 110716, 2021.

[132] S. Udayappan *et al.*, *Oral treatment with Eubacterium hallii improves insulin sensitivity in db/db mice. NPJ Biofilms Microbiomes 2: 16009*. 2016.

[133] P. W. Gilijamse *et al.*, 'Treatment with Anaerobutyricum soehngenii: a pilot study of safety and dose–response effects on glucose metabolism in human subjects with metabolic syndrome', *Npj Biofilms Microbiomes*, vol. 6, no. 1, p. 16, 2020.

[134] H. Tanno, T. Fujii, R. Ose, K. Hirano, T. Tochio, and A. Endo, 'Characterization of fructooligosaccharide-degrading enzymes in human commensal Bifidobacterium longum and Anaerostipes caccae', *Biochem. Biophys. Res. Commun.*, vol. 518, no. 2, pp. 294–298, 2019.

[135] L. A. Hesser *et al.*, 'A synbiotic of Anaerostipes caccae and lactulose prevents and treats food allergy in mice', *Cell Host Microbe*, 2024.

[136] T. Le Roy *et al.*, 'Dysosmobacter welbionis gen. nov., sp. nov., isolated from human faeces and emended description of the genus Oscillibacter', *Int. J. Syst. Evol. Microbiol.*, vol. 70, no. 9, pp. 4851–4858, 2020.

[137] T. Le Roy *et al.*, 'Dysosmobacter welbionis is a newly isolated human commensal bacterium preventing diet-induced obesity and metabolic disorders in mice', *Gut*, vol. 71, no. 3, pp. 534–543, 2022.

[138] E. M. de Hase *et al.*, 'Dysosmobacter welbionis effects on glucose, lipid, and energy metabolism are associated with specific bioactive lipids', *J. Lipid Res.*, vol. 64, no. 10, 2023.

[139] A. Mantri *et al.*, 'Beneficial Effects of Synbiotics on the Gut Microbiome in Individuals with Low Fiber Intake: Secondary Analysis of a Double-Blind, Randomized Controlled Trial', *Nutrients*, vol. 16, no. 13, p. 2082, 2024.

[140] A. M. Neyrinck *et al.*, 'Prebiotic dietary fibre intervention improves fecal markers related to inflammation in obese patients: Results from the Food4Gut randomized placebo-controlled trial', *Eur. J. Nutr.*, pp. 1–12, 2021.

[141] J. K. Oh *et al.*, 'Multispecies probiotics alter fecal short-chain fatty acids and lactate levels in weaned pigs by modulating gut microbiota', *J. Anim. Sci. Technol.*, vol. 63, no. 5, p. 1142, 2021.

Supplementary

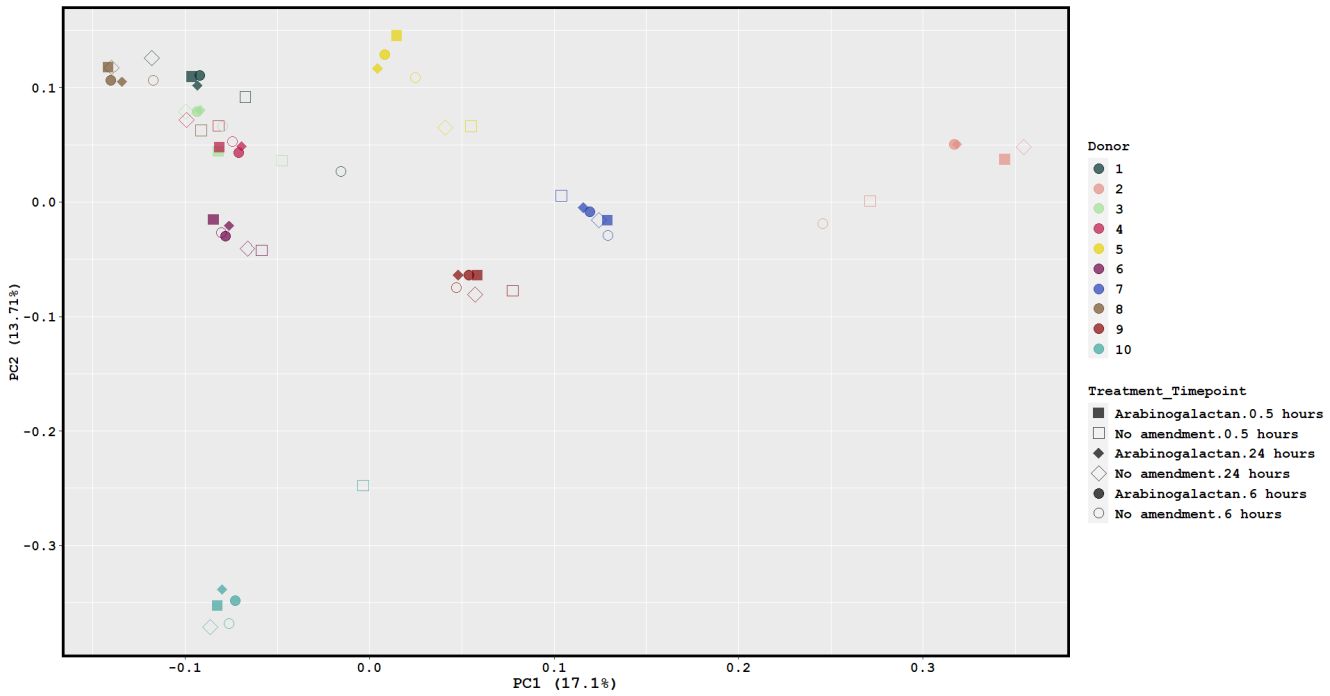

Figure S.1 Principal Component Analysis (PCA) of the whole microbial community of arabinogalactan (candidate prebiotic) and no amendment (control) treatments, across the three time points.

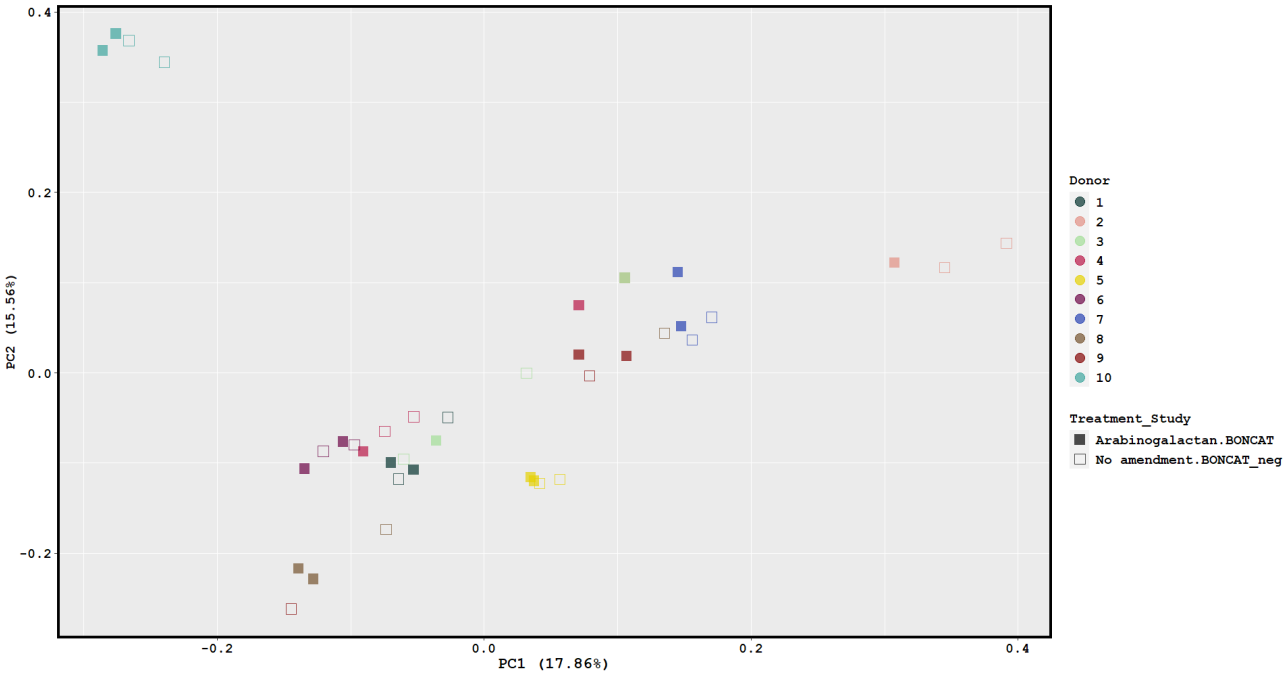

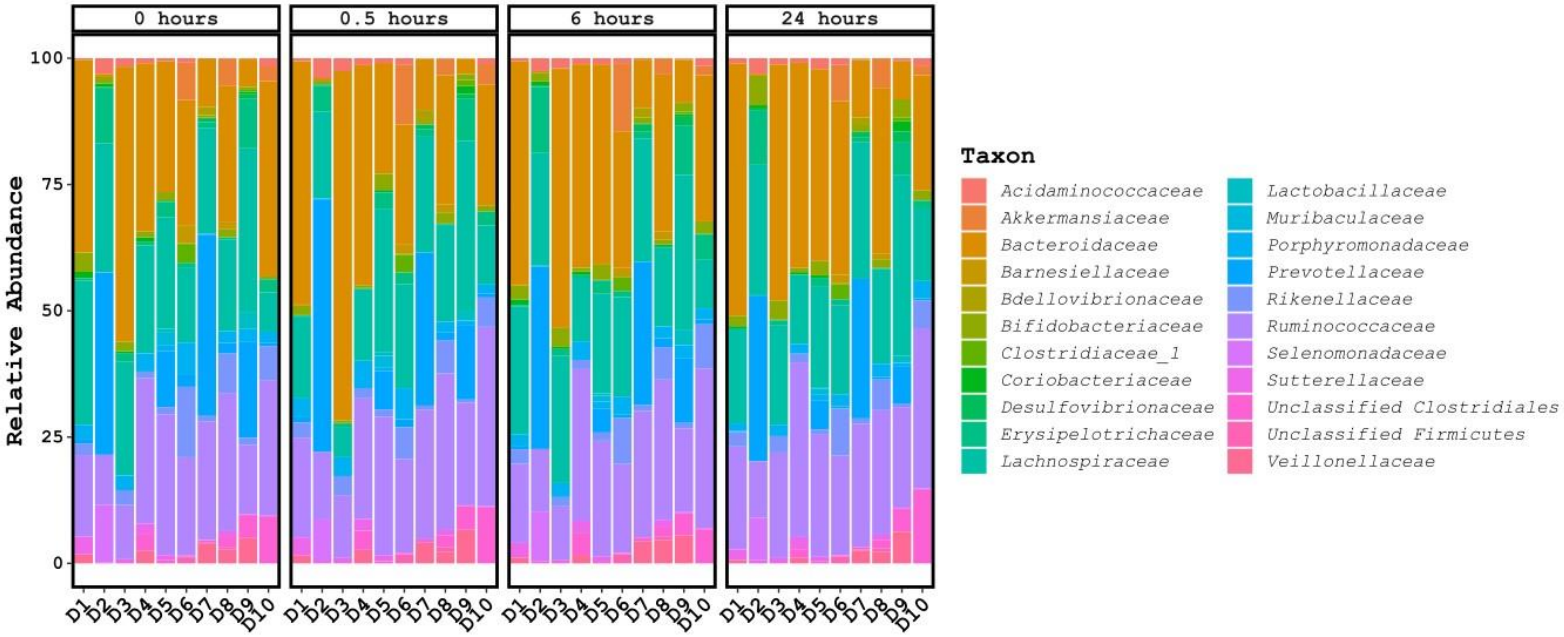

Figure S.3 Family level bacterial composition of microcosm samples during arabinogalactan (AG) treatment of all time points, compared with no amendment (NA) samples at 0.0h.

Zusammenfassung

Arabinogalactan (AG), ein Polysaccharid mit präbiotischem Potenzial, wurde hinsichtlich seiner Auswirkungen auf die Darmmikrobiota untersucht. Die Stuhlproben von 10 gesunden menschlichen Spendern wurden mithilfe moderner, kulturunabhängiger Techniken analysiert. Dazu gehörten Bioorthogonales Nicht-Kanonisches Aminosäure-Tagging (BONCAT) und Durchflusszytometrie (FACS), wobei L-Azidohomoalanin (AHA) als Marker für die Zellaktivität verwendet wurde. Zusätzlich kamen Raman-Mikrospektroskopie und Raman-aktiviertes Zellsortieren (RACS) mit schwerem Wasser (D_2O) zum Einsatz, um metabolisch aktive Bakterien zu verfolgen. AG beeinflusste sowohl die gesamte mikrobielle Gemeinschaft als auch den aktiven Anteil in anaeroben In-vitro-Inkubationen erheblich und förderte das Wachstum von Kommensalen und nützlichen Taxa wie *Bifidobacterium*, *Bacteroidetes*, *Faecalibacterium*, *Parabacteroides*, *Phascolarctobacterium* und *Blautia*. Trotz der interindividuellen Variabilität der Stoffwechselaktivität wurden über mehrere Gattungen hinweg konsistente Ergebnisse beobachtet. Die RACS-Analyse führte außerdem zur Isolierung einer breiten Palette von AG-abbauenden Stämmen, in Übereinstimmung mit früheren Ergebnissen, hauptsächlich aus den Gattungen *Bifidobacterium* und *Collinsella* sowie aus weiteren Gattungen wie *Alistipes*, *Bacteroides*, *Catenibacterium*, *Dysosmobacter*, *Eggerthella*, *Faecalibacterium*, *Parabacteroides*, *Phascolarctobacterium*, *Phocaeicola* und *Ruminococcus*. Darüber hinaus konnte gezeigt werden, dass AG das Wachstum von Mikroben fördert, die mit der Darmgesundheit, Immunmodulation und möglicherweise der kognitiven Funktion in Verbindung stehen, was Potenzial für zukünftige, gezielte therapeutische Anwendungen bietet. Diese Ergebnisse unterstreichen die Rolle von AG bei der Förderung nützlicher mikrobieller Populationen und unterstützen seine potenzielle Verwendung in der Entwicklung von Probiotika oder präbiotischen Nahrungsergänzungsmitteln der nächsten Generation. Weitere Studien zur Erforschung der Enzymaktivität und mikrobieller Interaktionen werden empfohlen, um die umfassenderen gesundheitlichen Auswirkungen von AG vollständig zu verstehen.